SANDIA REPORT
SAND2004-4813
Unlimited Release
Printed September 2004

Potential Application of Microsensor Technology in Radioactive Waste Management with Emphasis on Headspace Gas Detection

Yifeng Wang, Huizhen Gao, Robert C. Hughes, Clifford K. Ho, Michael L. Thomas, Jerome L. Wright, Lucas K. McGrath, Chad E. Davis, and Phillip I. Pohl

Prepared by
Sandia National Laboratories
Albuquerque, New Mexico 87185 and Livermore, California 94550

Sandia is a multiprogram laboratory operated by Sandia Corporation,
a Lockheed Martin Company, for the United States Department of Energy's
National Nuclear Security Administration under Contract DE-AC04-94AL85000.

Issued by Sandia National Laboratories, operated for the United States Department of Energy by Sandia Corporation.

Available to DOE and DOE contractors from
U.S. Department of Energy
Office of Scientific and Technical Information
P.O. Box 62
Oak Ridge, TN 37831

Telephone: (865)576-8401
Facsimile: (865)576-5728
E-Mail: reports@adonis.osti.gov
Online ordering: http://www.doe.gov/bridge

Available to the public from
U.S. Department of Commerce
National Technical Information Service
5285 Port Royal Rd
Springfield, VA 22161

Telephone: (800)553-6847
Facsimile: (703)605-6900
E-Mail: orders@ntis.fedworld.gov
Online order: http://www.ntis.gov/help/ordermethods.asp?loc=7-4-0#online

SAND2004-4813
Unlimited Release
Printed September 2004

Potential Application of Microsensor Technology in Radioactive Waste Management with Emphasis on Headspace Gas Detection

Yifeng Wang, Huizhen Gao, Robert C. Hughes, Clifford K. Ho, Michael L. Thomas, Jerome L. Wright, Lucas K. McGrath, Chad E. Davis, and Phillip I. Pohl

Sandia National Laboratories
P.O. Box 5800
Albuquerque, New Mexico 87185-0776

Abstract

Waste characterization is probably the most costly part of radioactive waste management. An important part of this characterization is the measurements of headspace gas in waste containers in order to demonstrate the compliance with Resource Conservation and Recovery Act (RCRA) or transportation requirements. The traditional chemical analysis methods, which include all steps of gas sampling, sample shipment and laboratory analysis, are expensive and time-consuming as well as increasing worker's exposure to hazardous environments. Therefore, an alternative technique that can provide quick, in-situ, and real-time detections of headspace gas compositions is highly desirable. This report summarizes the results obtained from a Laboratory Directed Research & Development (LDRD) project entitled "Potential Application of Microsensor Technology in Radioactive Waste Management with Emphasis on Headspace Gas Detection". The objective of this project is to bridge the technical gap between the current status of microsensor development and the intended applications of these sensors in nuclear waste management. The major results are summarized below:

- A literature review was conducted on the regulatory requirements for headspace gas sampling/analysis in waste characterization and monitoring. The most relevant gaseous species and the related physiochemical environments were identified. It was found that pre-concentrators might be needed in order for chemiresistor sensors to meet desired detection limits.
- A long-term stability test was conducted for a polymer-based chemresistor sensor array. Significant drifts were observed over the time duration of one month. Such drifts should be taken into account for long-term in-situ monitoring.

- Several techniques were explored to improve the performance of sensor polymers. It has been demonstrated that freeze deposition of black carbon (CB)-polymer composite can effectively eliminate the so-called “coffee ring” effect and lead to a desirable uniform distribution of CB particles in sensing polymer films. The optimal ratio of CB/polymer has been determined. UV irradiation has been shown to improve sensor sensitivity.
- From a large set of commercially available polymers, five polymers were selected to form a sensor array that was able to provide optimal responses to six targetvolatile organic compounds (VOCs). A series of tests on the response of sensor array to various VOC concentrations have been performed. Linear sensor responses have been observed over the tested concentration ranges, although the responses over a whole concentration range are generally nonlinear.
- Inverse models have been developed for identifying individual VOCs based on sensor array responses. A linear solvation energy model is particularly promising for identifying an unknown VOC in a single-component system. It has been demonstrated that a sensor array as such we developed is able to discriminate waste containers for their total VOC concentrations and therefore can be used as screening tool for reducing the existing headspace gas sampling rate.
- Various VOC preconcentrators have been fabricated using Carboxen 1000 as an absorbent. Extensive tests have been conducted in order to obtain optimal configurations and parameter ranges for preconcentrator performance. It has been shown that use of preconcentrators can reduce the detection limits of chemiresistors by two orders of magnitude. The life span of preconcentrators under various physiochemical conditions has also been evaluated.
- The performance of Pd film-based H_2 sensors in the presence of VOCs has been evaluated. The interference of sensor readings by VOC has been observed, which can be attributed to the interference of VOC with the H_2-O_2 reaction on the Pd alloy surface. This interference can be eliminated by coating a layer of silicon dioxide on sensing film surface.

Our work has demonstrated a wide range of applications of gas microsensors in radioactive waste management. Such applications can potentially lead to a significant cost saving and risk reduction for waste characterization.

Contents

List of Figures

List of Tables

1. Introduction

Waste characterization is probably the most costly part of radioactive waste management. For example, transuranic wastes destined to the Waste Isolation Pilot Plant (WIPP) alone could cost billions of dollars for characterization. As an important part of this characterization, the measurements of headspace gas in waste containers are generally required for the demonstration of compliance with Resource Conservation and Recovery Act (RCRA) or transportation requirements. The gases to be measured include various volatile organic compounds (VOCs) and flammable hydrogen gas (H_2). The current measurements, which are based on a traditional chemical analysis approach, need to go through all steps of gas sampling, sample shipment, and laboratory analysis. Since they are usually required for each individual waste container (this is the case for WIPP wastes), such measurements are expensive and time-consuming as well as increasing worker's exposure to hazardous environments. Therefore, an alternative gas detection technique is highly desirable for both cost saving and risk reduction.

Sandia National Laboratories have developed various microsensors for detecting organic solvent vapors and hydrogen gas (e.g., Ricco et al., 1998; Patel et al., 2000; Hughes et al., 1989, 1994). With appropriate further development and adaptation, such sensors can potentially have a wide range of applications in radioactive waste characterization. For instance, the current characterization of transuranic wastes generally requires headspace gas sampling and analysis for every waste container. In this case, a quick and on-site detection of headspace gases using microsensors can allow a significant reduction in the sampling rate because microsensors can quickly screen whether a specific waste drum contains a high VOC concentration and therefore needs a further analysis. Microsensors can also be applied to other parts of nuclear waste management such as VOC monitoring in interim waste storage facilities or permanent disposal rooms, for which microsensors can provide real-time and in-situ measurements that otherwise are difficult to obtain.

This report summarizes the results obtained from a Laboratory Directed Research & Development (LDRD) project entitled "Potential Application of Microsensor Technology in Radioactive Waste Management with Emphasis on Headspace Gas Detection". The objective of this project is to bridge the technical gap between the current status of microsensor development and the intended applications in nuclear waste management. Specifically, the project is intended to address the following issues:

- Long-term stability of microsensors and possible improvements: Microsensors must be tested for their long-term performance (e.g. drift) under physiochemical conditions anticipated in waste containers, especially for possible interference from coexisting chemical components.
- Ability of VOC microsensors for the discrimination of individual compounds: Multiple VOCs may be present in radioactive wastes, and microsensor arrays must be maximized for their capability of differentiating individual VOCs.
- Feasibility of using microsensors as a screening tool to discriminate two populations of waste containers according to a pre-specified total (not individual) VOC concentration limit. A high reading could be used to point to barrels that need further investigation. In some cases, it is also desired for microsensors to be able to indicate the presence of an anomaly compound that does not belong to a specified group of VOCs.

Various types of gas microsensors have been developed based on different detection methods (Ho et al., 2001). To limit the work scope of the project, however, we have chosen to focus our research exclusively on chemiresistor microsensors and their applications in the characterization of transuranic wastes. Each of these sensors consists of an array of chemiresistors. Each chemiresistor is made by coating a planar interdigitated electrode array with a thin film of a specific polymer loaded with conductive particles (Hughes et al., 2000). When a gaseous chemical compound comes into contact with the chemiresistor, the polymer reversibly absorbs the chemical and swells, thus changing the resistance of the film that can be measured. The change in resistance is a function of the amount of the chemical compound absorbed, which is in turn determined by the concentration of that compound in the gas phase. Different polymers may have different tendencies for absorption of a targetcompound. By integrating an array of chemiresistors on a single of chip, a microsensor can in principle identify and quantify, at least to some extent, different VOCs by measuring resistance changes of each chemiresistor.

Table 1. Regulatory concentration limits for H_2 and nine volatile organic compounds (VOCs) in transuranic wastes and detection limits of gas microsensors. VOC concentrations are in ppmv.

Volatile Organic Compound	Regulatory Concentration Limit	Typical Headspace Concentration in waste stream	Detection limit of microsensor[1]	Detection limit of microsensor with pre-concentrator[2]
Carbon tetrachloride	9,625	0.1 – 1,230[3]	120	1
Chlorobenzene	13,000	0 - 260	10	< 1
Chloroform	9,930	0 - 280	210	2
1,1-Dichloroethane	5,490	0 - 240	240	2
1,2-Dichloroethane	2,400	0 - 230	110	1
Methylene chloride	100,000	0.3 - 2550	460	5
1,1,2,2-Tetrachloroethane	2,960	0.2 - 230	10	< 1
Toluene	11,000	0.4 - 360	30	< 1
1,1,1-Trichloroethane	33,700	8 - 6590	130	1
H_2	5%	0 - >5%	10 ppmv - 0.1%	

[1] Detection limits of VOC microsensors are usually about 0.1% of VOC vapor pressures. The actual detection limits of VOC sensors need to be tested.

[2] Use of a pre-concentrator could reduce the detection limits by a factor of ~100.

[3] For solidified organics waste streams, the concentrations of carbon tetrachloride could be >3,340.

To establish an appropriate set of boundary conditions for sensor testing, an extensive literature review has been conducted on the relevant regulatory requirements for headspace gas sampling and analysis in transuranic waste characterization. The most relevant gaseous species in the wastes have been identified, and their typical concentration ranges and regulatory limits have been constrained as compared to the possible detection limits of typical chemiresistor microsensors (Table 1). From Table 1, it is expected that a pre-concentrator, which is used to

improve detection limits, may be required for the needed accuracy in waste characterization. Through the literature search, the relevant physiochemical conditions for microsensor testing experiments have also been defined: humidity (0 - 100%), temperature (< 60 ^{o}C), varying O_2, HCl and CH_4 concentrations, and dusty environments.

This report is organized as follows:

Section 1.0 Introduction (Contributor: Wang)
Section 2.0 Chemiresistor Sensors for VOC Detection (Contributors: Gao, Wang, and Ho)
Section 3.0 Development of Preconcentrators for VOC Detection (Contributors: Thomas and Wright)
Section 4.0 Hydrogen Sensors (Contributor: Hughes)
Section 5.0 Summary (Contributor: Wang)

2. Chemiresistor Sensors for VOC Detection

2.1 Polymer-Based Chemiresistor Sensors

Chemiresistor sensors detect volatile organic compound (VOC) vapors via conductive polymer films that are deposited onto micro-fabricated circuits (Hughes et al., 2000). A chemically sensitive polymer is dissolved in a solvent and mixed with conductive carbon particles (carbon black). The resulting ink is then deposited and dried onto thin-film platinum traces on a solid substrate (chip). When a VOC vapor comes into contact with the polymer, the VOC absorbs into the polymer, causing it to swell. The swelling changes the resistance of the polymer film, which can be measured and recorded using a data logger or an ohmmeter (Figure 1). The swelling is reversible if the VOC is removed, but some hysteresis may occur at high concentration exposures. The amount of swelling corresponds to the concentration of the VOC in contact with the chemiresistor, and so each resistor can be calibrated by exposing the chemiresistors to known concentrations of target analytes. Additional information regarding the fabrication and calibration of chemiresistor sensors can be found in Ho et al. (2002, 2003).

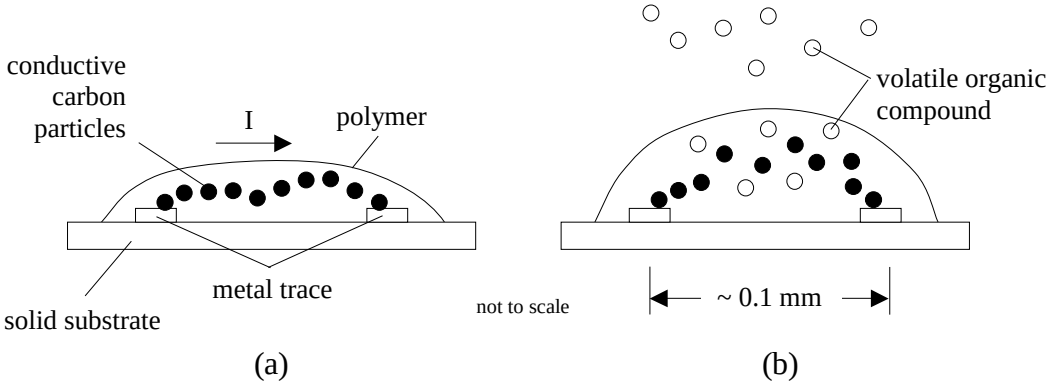

Figure 1. VOC detection by a thin-film chemiresistor: (a) Electrical current (I) flows across a conductive thin-film carbon-loaded polymer deposited on a micro-fabricated electrode; (b) VOCs absorb into the polymer, causing it to swell (reversibly) and break some of the conductive pathways, which increases the electrical resistance.

Figure 2 shows the architecture of a microsensor, which integrates an array of chemiresistors with a temperature sensor and heating elements (Hughes et al., 2000; Ho et al., 2003). The chemiresistor array has been shown to detect a variety of VOCs including aromatic hydrocarbons (e.g., benzene), chlorinated solvents (e.g., trichloroethylene (TCE), carbon tetrachloride), aliphatic hydrocarbons (e.g., hexane, isooctane), alcohols, and ketones (e.g., acetone). The on-board temperature sensor comprised of a thin-film platinum trace can be used to not only monitor the in-situ temperature, but it can also provide a means for temperature control. A feedback control system between the temperature sensor and on-board heating

elements can allow the chemiresistors to be maintained at a fairly constant temperature, which can aid in the processing of data when comparing the responses to calibrated training sets. In addition, the chemiresistors can be maintained at a temperature above the ambient to prevent condensation of water, which may be detrimental to the wires and surfaces of the chemiresistor.

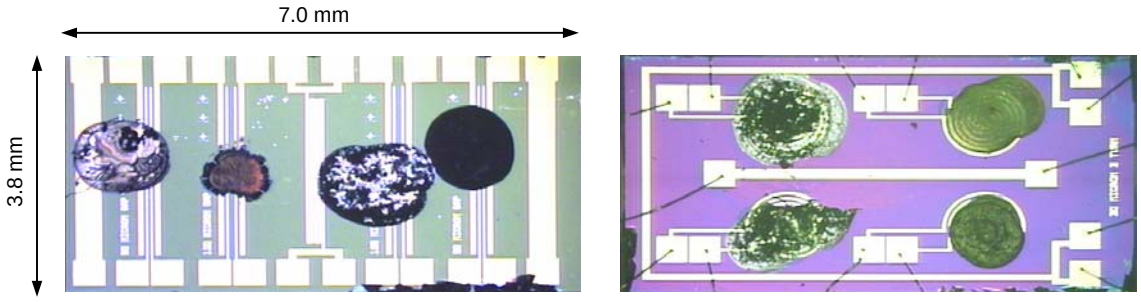

Figure 2. Chemiresistor arrays with four conductive polymer films (black spots) deposited onto a micro-fabricated circuit. Left: Linear-electrode design (C4) with a temperature sensor in the middle and heating elements on the ends. Right: New spiral-electrode design (E2) with temperature sensor on the perimeter and heating element in the middle.

A robust package has been designed and fabricated to house the chemiresistor array (Ho and Hughes, 2002). This cylindrical package is small (~ 3 cm diameter) and is constructed of rugged, chemically resistant material. Early designs have used PEEK (PolyEtherEtherKetone), a semi-crystalline, thermoplastic with excellent resistance to chemicals and fatigue. Newer package designs have been fabricated from stainless steel (Figure 3). The package design is modular and can be easily taken apart (unscrewed like a flashlight) to replace the chemiresistor sensor if desired. Fitted with Viton O-rings, the package is completely waterproof, but gas is allowed to diffuse through a GORE-TEX® membrane that covers a small window to the sensor. Like clothing made of GORE-TEX®, the membrane prevents any liquid water from passing through it, but the membrane "breathes," allowing vapors to diffuse through. Mechanical protection is also provided via a perforated metal plate that covers the chemiresistors. The chemiresistors are situated on a 16-pin dual-in-line package that is connected to a weatherproof cable. The cable can be connected to a hand-held multimeter for manual single-channel readings, or it can be connected to a multi-channel data logger for long-term, remote operation.

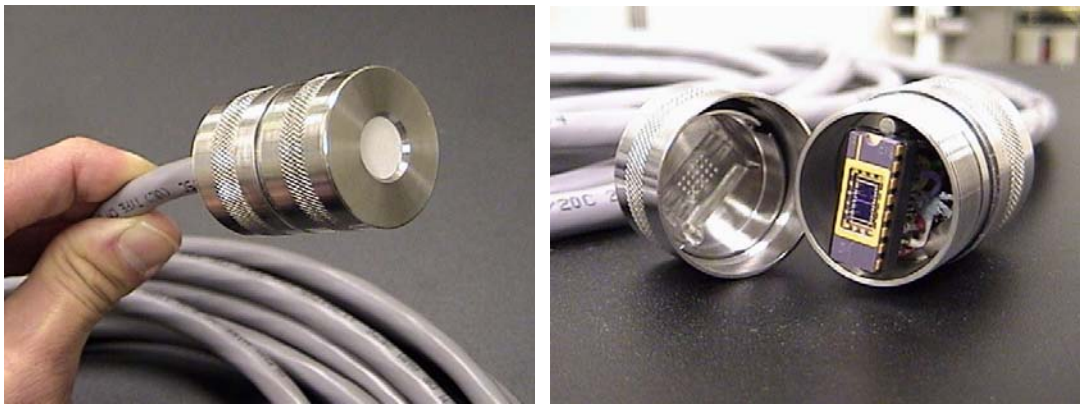

Figure 3. Stainless-steel waterproof package that houses the chemiresistor array. Left: GORE-TEX® membrane covers a small window over the chemiresistors. Right: Disassembled package exposing the 16-pin dual-in-line package and chemiresistor chip.

2.2 Long-Term Stability Testing

For in-situ VOC monitoring in a waste container or a waste disposal facility, it is desirable that microsensors can continuously provide reliable measurements over a long time period with as few calibration events as possible. This section summarizes the results of long-term stability tests for a set of sensing polymers commonly used in microsensors.

A chemiresistor array was exposed continuously to trichloroethylene (TCE) for over a month to evaluate the stability of the polymers during an extended period of continuous exposure. The chemiresistor array consisted of poly(N-vinyl pyrolidone) (PNVP), (poly(epichlorohydrin) (PECH), poly(ethylene-vinyl acetate) (PEVA), and poly(isobutylene) (PIB). PNVP is a polar polymer that responds well to water vapor, and the other three polymers respond well to various organics. The chemiresistor array was placed inside a steel tube that was connected to a gas bottle containing a fixed concentration of TCE at 1000 parts per million by volume (ppmv) (Figure 4). The TCE was allowed to flow through the tube for 30 minutes to ensure that the gas inside the tube reached 1000 pppm. The tube was then sealed with the chemiresistor array inside, and the response of the chemiresistor array was monitored for 33 days. On the last day, dry air was passed through the tube for about an hour to re-establish a "dry-air" baseline, and then 1000 ppmv of TCE was introduced again for about an hour. Figure 5 shows the resistance of each of the four polymers during the test.

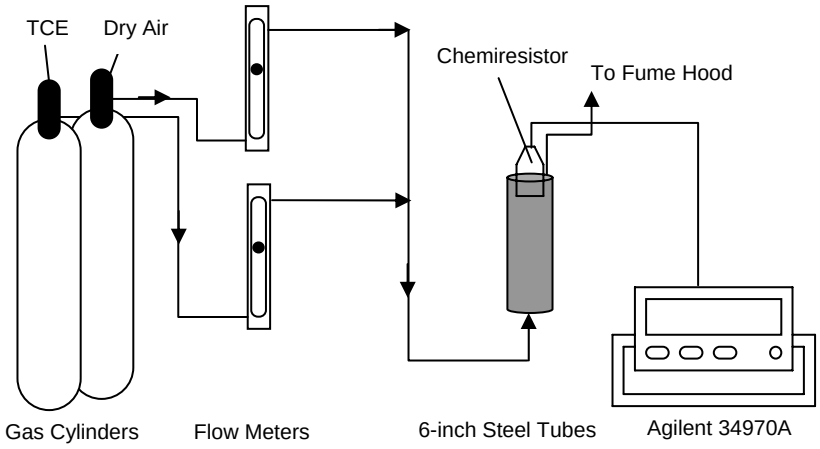

Figure 4. Schematic of experimental apparatus used for long-term exposure study.

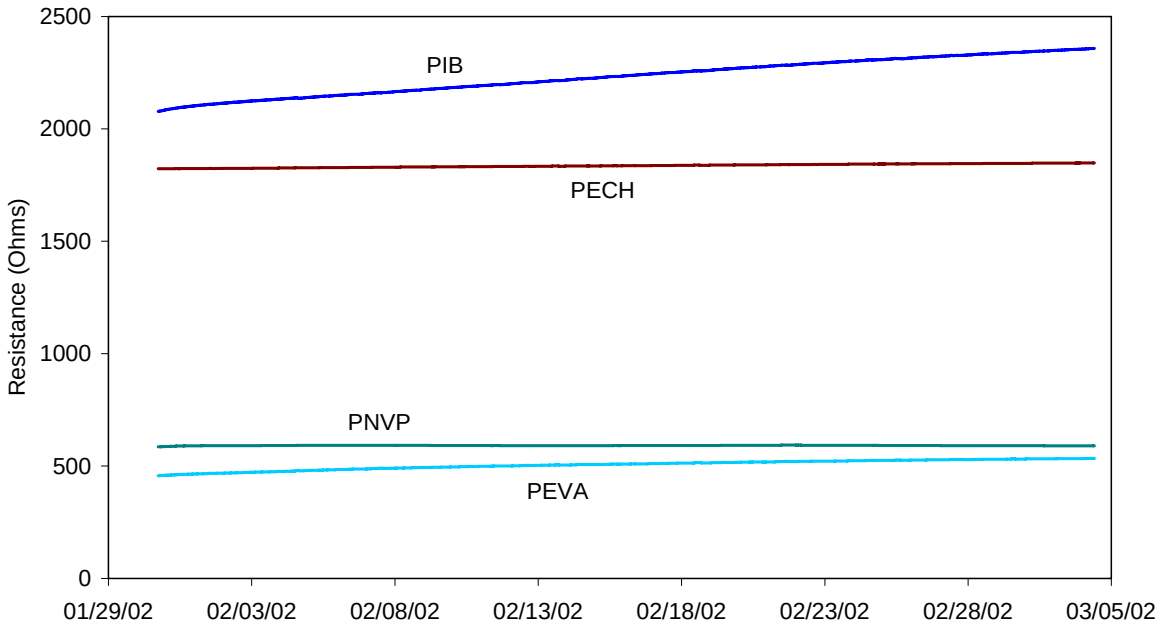

Figure 5. Measured resistances of chemiresistor polymer array during 33 days of exposure to 1000 ppmv of TCE.

Figure 6 shows the relative change in resistance (ΔR/R) for each of the polymers. The relative change in resistance is generally used in calibrations to mitigate the variability in the initial baseline resistance of each polymer (Ho et al., 2003). The response of PEVA, PIB, and, to a lesser degree, PECH, all show that there is a long-term drift in the response of the polymers. The polar polymer, PNVP, which responds to changes in water vapor concentration, did not fluctuate significantly. If leaks were present, water vapor from the ambient would diffuse into the tube and increase the water-vapor concentration (and therefore the resistance of PNVP) inside the "dry" tube (the TCE originating from the gas bottle was mixed with nitrogen). Therefore, the relative constant response of PNVP indicates that the tube containing the chemiresistor array was well sealed and no gas exchange took place between the interior of the tube and the ambient during the test. Therefore, the relative resistance changes observed for PEVA and PIB are the long-term drifts.

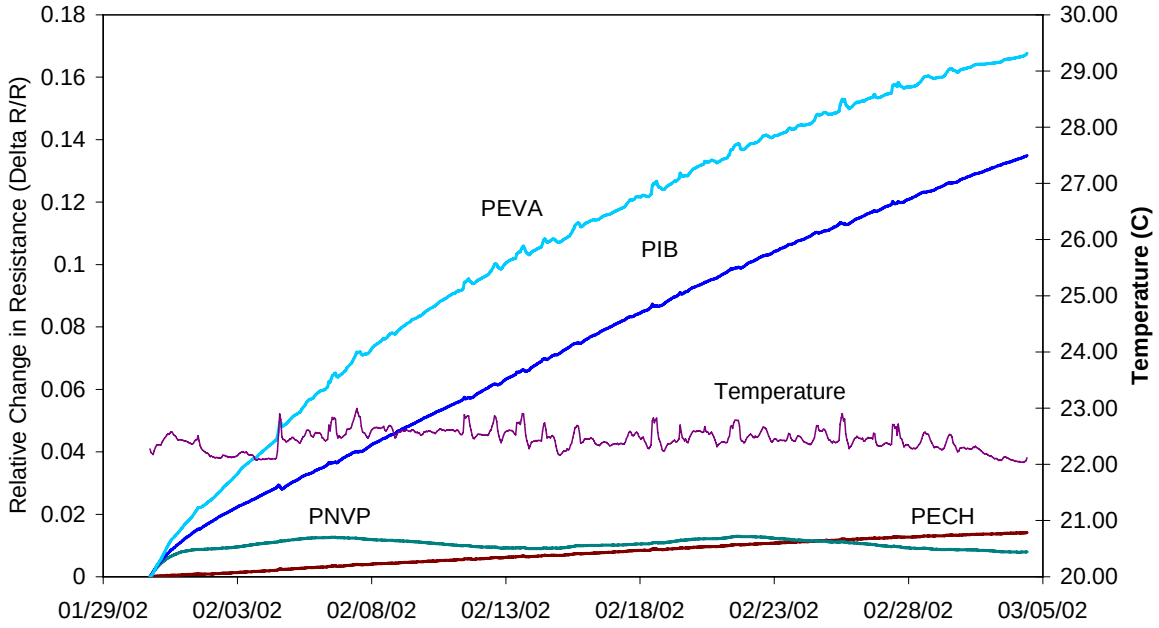

Figure 6. Relative change in resistance of the four chemiresistor polymers during the 33-day exposure to 1000 ppmv of TCE.

The total drifts are significant when compared to the change encountered when exposed to 1000 ppm of TCE for one hour (using dry air as a baseline) (Figure 7). The relative change during the 33 days of exposure is over an order of magnitude greater than the short-term change when exposed to 1000 ppmv of TCE. As discussed in Section 2.5, however, the long-term drifts of the sensors can be greatly reduced by modifying the procedure for polymer film deposition.

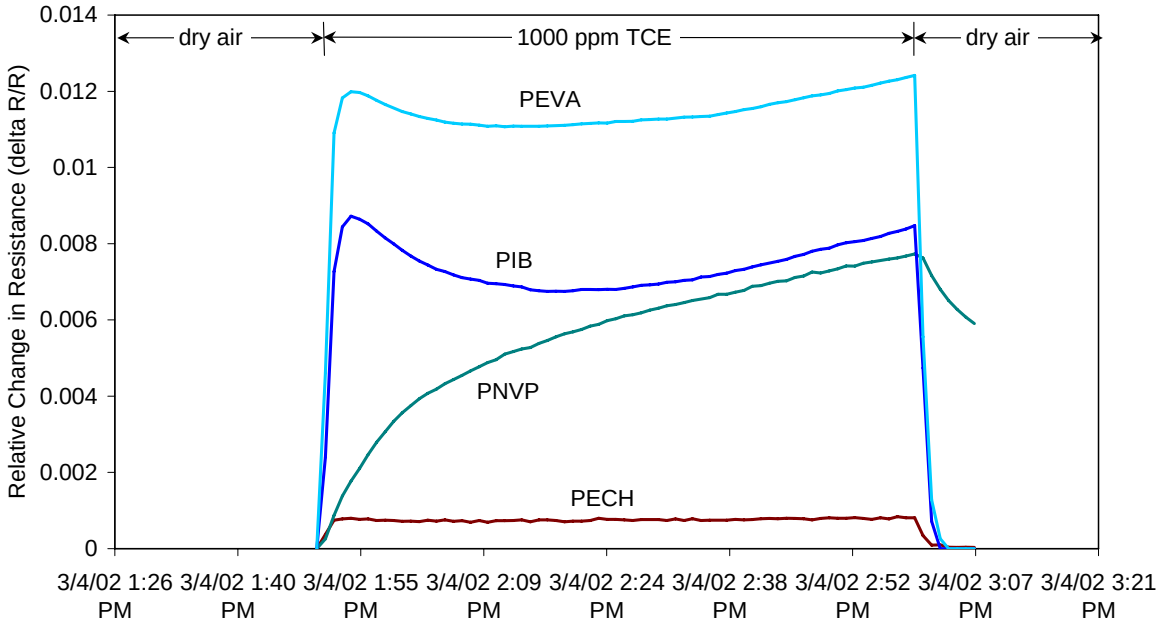

Figure 7. Relative change in resistance of the four sensing polymers during a one-hour exposure to 1000 ppmv of TCE after being exposed to dry air.

2.3 Selection and Optimization of Polymer-Carbon Composites

As mentioned above, a sensing polymer is prepared by mixing carbon black (CB) and polymer in an appropriate solvent. The mixture is then deposited on the substrate between two metal electrodes, whereby the solvent evaporates leaving a composite film. This section discusses the selection of polymers and the optimization of carbon black/polymer ratios in order to maximize a chemiresistor array for detection and discrimination of individual VOCs.

2.3.1 Deposition of Polymer-Carbon Black Film

A certain amount of a selected polymer (0.1 g) was mixed with an appropriate solvent (5 mL) in a vial. The solvent was chosen so that it had a high solubility for the polymer. Solvents chosen for dissolving specific polymers are listed in Table 2. The vial was then placed on a hot plate at approximately 40 ^{o}C and shaken occasionally. After the dissolution was completed a certain quantity of carbon black was added to the polymer/solvent mixture. The vial was then place in an ultrasonic cleaner and sonicated for an hour to disperse the carbon black into the polymer/solvent mixture. The ink was finally ready for deposition on dies.

Table 2. List of Solvents for Dissolving Specific Polymers

Polymer	Solvent
Ethylene/Vinyl acetate copolymer (PEVA)	1,1,1-Trichloroethane (TCA)
Polystyrene (PS)	Toluene
Styrene/Ethylene-Butylene, ABA copolymer (ScEB)	Toluene
Vinyl chloride/Vinyl acetate/Hydroxypropyl acrylate terpolymer (VCVAHPA)	Toluene
Zein	90% Ethanol

The dies were cleaned with acetone or methanol. A micropipette was placed inside the vial that was kept sonicated. A small amount of ink wicked up into the micropipette. The micropipette was then placed directly above the area for deposition, and a small pressure was applied on the micropipette to push a drop of ink out of the pipette. The tip of micropipette was gently touched on the chip and then quickly lifted. The resistance of the deposit was measured with an electric multimeter (FLUKE 87 III, TRUE RMS). If no current was measured, more ink was applied or the prior deposition could be wiped off with acetone followed by another deposition. A sensing polymer film was finally formed after the solvent evaporated.

2.3.2 Selection of Sensing Polymers

To detect a specific VOC, it would be ideal to design a polymer that has a high selectivity for the targetanalyte, the methology generally referred to a “lock-and-key” approach. In practice, however, this is hard to achieve. Instead, we use an array of sensing polymers that preferably have different (but not necessarily exclusive) responses to different VOCs. An individual VOC is then identified by collectively analyzing signals from all sensing polymers in the sensor array. Therefore, the selection of an appropriate set of polymers is the key to the sensor performance.

In principle, the selection of a sensing polymer can be guided by the solubility parameters that characterize the affinity of a specific polymer to a VOC to be detected (Eastman et al., 1999). A polymer with a high solubility for the analyte is generally chosen. To form a sensor array, the chosen polymers should also be diverse in their functional groups and structures so that the responses of the sensor array can provide a unique fingerprint for individual VOCs. Thirty polymers from the polymer kit (SP^2) were originally selected for further screening. Each polymer was dissolved in an appropriate solvent and then mixed with carbon black (PRINTEX XE2) from Degussa at the CB/polymer ratio of 20% (w/w). A high-intensity ultrasonic processor (Autotune series 500 Watt model, Sonicsandmateria, in the pulse mode, 2.5s/1s on/off) was used to disperse carbon black particles into the polymer without overheating the system.

Two μL of the polymer-CB composite were deposited on a circuit board, which was immediately moved onto a block of dry ice after the deposition. Each board was loaded with 10 polymer-CB composites. The circuit board was then wired and placed in a sealed canister, which was repeatedly injected with an individual VOC vapor and subsequently purged with N_2 gas during testing. The resistance changes of each sensing polymer were measured with an Agilent Data Acquisition/Switch unit (34970A, Agilent Technologies, Inc.). Figure 8 shows the experimental setup for the testing.

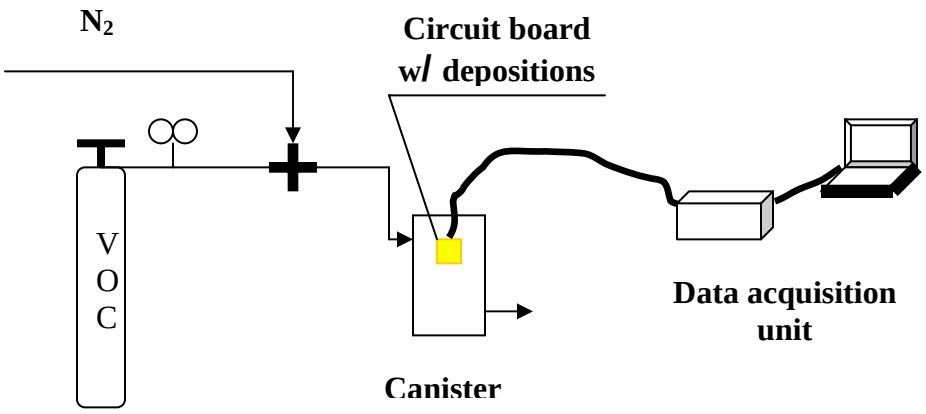

Figure 8. Experimental setup for screening sensing polymers

From thirty polymers tested from different categories, five polymers were finally selected to form a chemiresistor array (Table 1): Ethylene/Vinyl acetate copolymer (PEVA), Polystyrene (PS), Styrene/Ethylene-Butylene, ABA copolymer (ScEB), Vinyl chloride/Vinyl acetate/ Hydroxypropyl acrylate terpolymer (VCVAHPA), and Zein. These polymers were selected according to both the sensitivity of their responses and the capability for differentiating individual VOCs. For example, as shown in Figure 9, PEVA and PS both are sensitive to toluene but response differently to TCA.

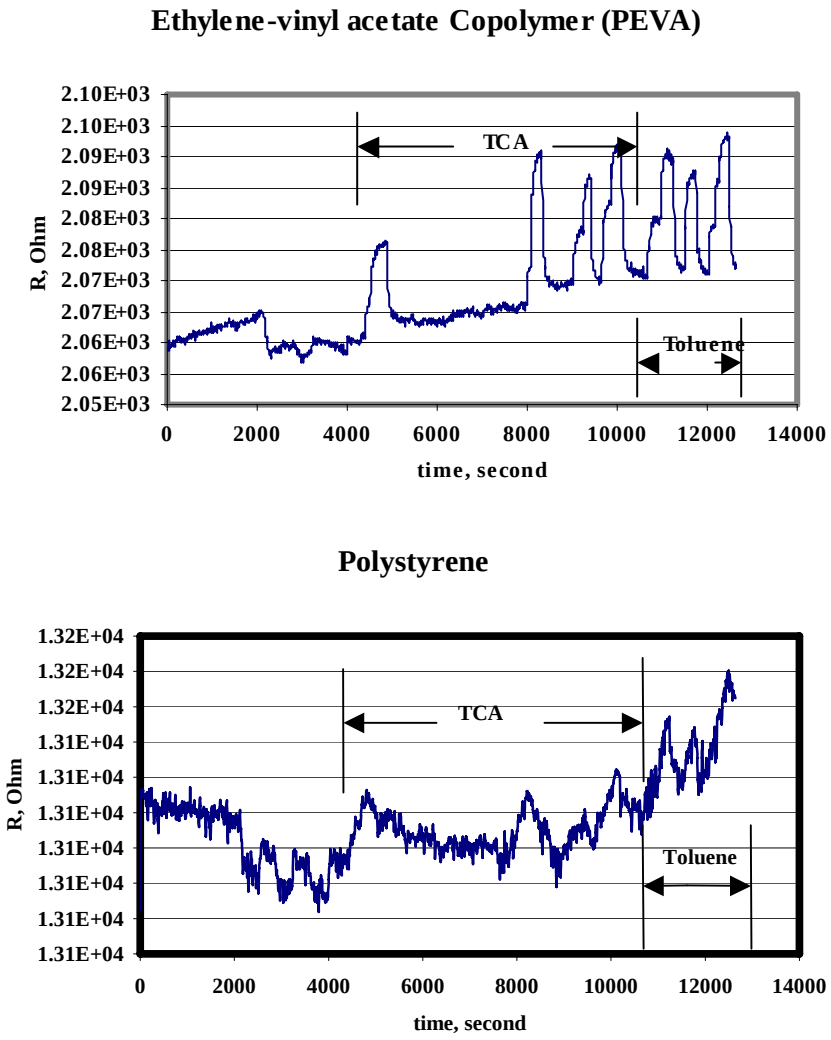

Figure 9. Responses of ethylene/vinyl acetate copolymer (PEVA) and polystyrene (PS) to trichloroethane (TCA) and toluene. Note that the two polymers display different response characteristics.

2.3.3 Selection of Carbon Black

Polymers and organic solvents are generally excellent electrical insulators. However, when a polymer is mixed with carbon black at a concentration above a threshold (the electrical percolation concentration), the composite becomes relatively a good electrical conductor. Thus, the carbon black imparts the main electrical characteristics of the composite. The physical properties of the CB particles, the CB mass loading in the composite and the distribution of CB particles directly affect the conductivity of the composite and the overall performance of the sensing polymer. The aspects of carbon black morphology that have been considered include particle size, porosity, number of particles per aggregate, openness/clustering, anisometry and

distribution of these properties (Medalia, 1985). Nano-scale carbon black particles distributed evenly in the polymer branched structure could provide better adhesion to polymer chains compared to microspheres or their aggregates. Knite and his co-workers (Knite et al. 2002) have studied carbon black polymeric nanocomposite on both macro- and nano-scales to examine the reversible tensoresistive effect of electric resistance dependence using an extra conductive carbon black (PRINTEX XE2, DEGUSSA), which has the primary particle diameter of 35 nm (max.). We have compared this material with the carbon black from PolyScience in terms of the sensitivity and stability of the resulting polymer-CB composites. The results are shown in Table 3. It is clear that PRINTEX XE2 carbon black provides a better performance (i.e., lower baseline shift) than Polyscience CB. Therefore, we have chosen to use the PRINTEX XE2 carbon black material.

Table 3. Comparison of sensing polymer composites with different carbon blacks. The composites contain 40 wt% carbon black and are prepared at a room temperature.

Carbon black source	PolyScience		Degussa XE2	
Operation*	Baseline shift (slope)	Resistance, (Ohm)	Baseline shift (slope)	Resistance, (Ohm)
Pre - eq.	0.1329	1700	1E-0.5	187
NaCl – eq.	0.1731	3692	6E-05	187
N_2 Purging	0.1185	400		188

(Note *: pre-eq. stands for equilibration in the air; NaCl-eq. stands for equilibration with 75% relative humidity over a NaCl-saturated solution; purging stands for the responses to alternated trichloroethane(TCA) and N_2 purging.)

2.3.4 Optimization of Carbon Black/Polymer Ratio

When an insulating polymer mixed with carbon-black particles, above a certain CB concentration, electro-conductive channels are formed in the polymer matrix. The inter-aggregate conduction has been attributed to the overlap of wave functions across conductive particles (Medalia, 1985). No matter what kind mechanism used for deciphering the electric behavior of the composite, it is obvious that the distance between the CB particles is a major factor influence the conductivity. On one hand, too low CB loadings (i.e., too large separations among conductive particles) may result in too low conductivities of the composites and high noise/signal ratios. On the other hand, as the CB loading approaches a saturated concentration (p_s), the change in conductivity (σ) becomes insensitive to CB loading (p) (Figure 10). The effect of CB loading on the conductivity of a CB-polymer composite near the critical concentration can be described within the framework of percolation theory (Foulger, 1999):

$$(p \quad p_c)^n \qquad (1)$$

where is the change in conductivity; p_c is the volume fraction of carbon black (p) at the percolation threshold; and n characterizes the scaling behavior in the region near p_c.

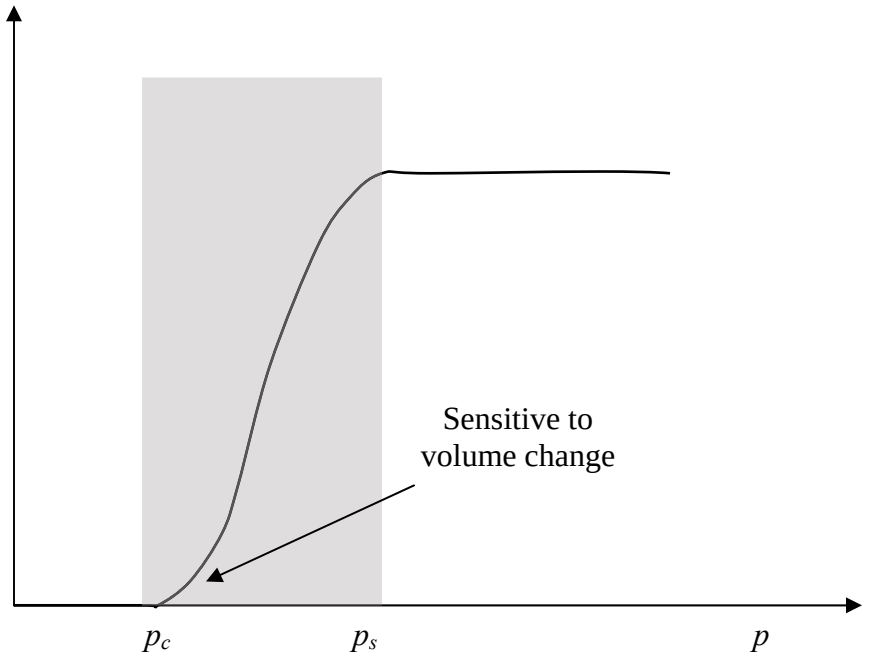

Figure 10. Schematic diagram showing the conductivity c h a n g e o f e r a composite as a function of CB loading

In order to obtain an optimal CB concentration for sensor performance, we tested four mas s l o a d i n g s o f composites: 3, 10, 20, and 40 wt % CB. The results are shown in Figure 11. It is shown in the figure that the percolation threshold of CB concentration falls in the r a n g e o f 3 - 1 0 w t % can be obtained when CB concentrations are r e s p o n close to the percolation threshold, where a small volume expansion would give rise to a large resistance change (Figure 10). Experimental data have shown that the composite with 3 wt % of CB has the highest relative resistance change (i.e., the highest sensitivity) as well as the highest noise/signal ratio. For our work, we have chosen 10 – 20 wt % as optimal CB concentrations.

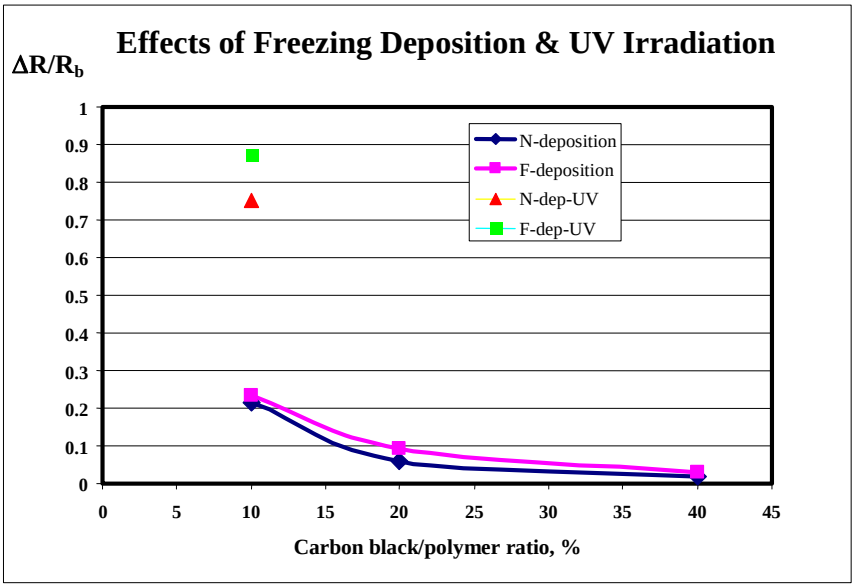

Figure 11. Effects of CB loading, drying temperature, and UV irradiation on the sensitivity of PEVA-CB composites in response to trichloroethane (TCA) sorption. The data for 3 wt % CB is not shown here because of a too high noise/signal ratio.

2.3.5 Uniform Distribution of CB Particles

The actual distribution of CB particles within the sensing polymer film directly impacts sensor performance. A uniform distribution of the particles is generally required for sensors to provide good responses. The traditional methods for preparing sensing polymer films have an inherent drawback. Optical microscopic observations have revealed that the polymer films prepared with these methods are generally heterogeneous in CB particles distribution with CB particles concentrated on the rim of the film domain, forming a so-called "coffee ring". This "coffee ring" effect has been attributed to the preferential movement of CB particles during solvent evaporation (Deegan et al. 2000; Gonuguntla & Sharma 2004). As shown in Figure 12, the sharp point between the solution droplet at the edge and the substrate causes a very large increase in the evaporation rate. This increased evaporation at the edge forces the solvent to move to the rim, carrying suspended solid particles and depositing them at the edge.

To eliminate the "coffee ring" effect, we have developed a freeze deposition method for preparing sensing polymer films. The central idea of this method is to keep the CB-polymer suspension below the freezing temperature during the evaporation of solvent, therefore completely eliminating the possibility for liquid movement. In our experiments, we used dry ice (CO_2) purchased from a grocery store. The microchip was first placed on a dry-ice block. Immediately before the deposition of polymer film, the surface of the chip was wiped off with a

Q-tip to remove condensed water vapor. After the deposition, the chip remained on the dry ice until the solvent completely evaporated. The results are shown in Figure 13. The left side circuits in the figure were deposited under ambient temperature (~24 ^{o}C). The right side circuits were deposited over dry ice (-78.5 ^{o}C). Carbon black rings are clearly seen on the left side circuits, which were dried under a room temperature. In contrast, the polymer films deposited over dry ice show uniform distributions of CB particles. Note that the same CB/polymer ratios were used for all circuits shown in the figure.

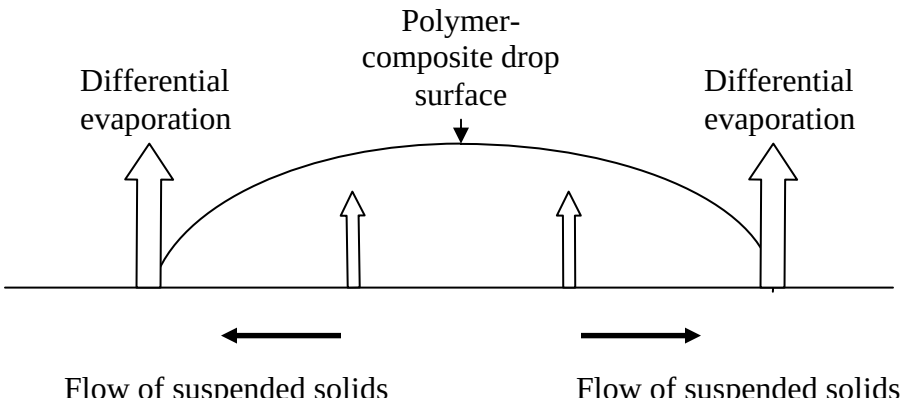

Figure 12. Schematic diagram of differential evaporation resulting in the formation of "coffee rings"

Our experimental data have also shown that the freeze-deposition method can significantly improve sensor performance. The sensing polymer films prepared with freeze deposition display a relative low resistance, and the baseline drift is reduced by a factor of 20.

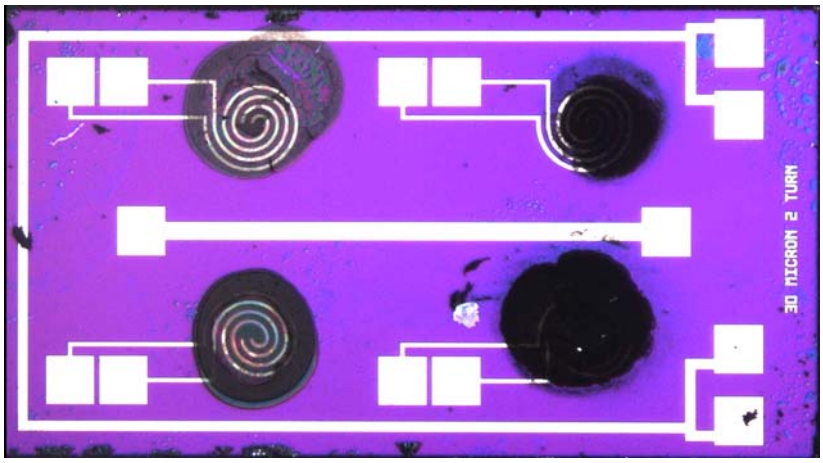

Figure 13. CB particle distributions with sensing polymer films prepared with different deposition methods. The left panel was deposited at room temperatures and the right panel was prepared with freeze deposition.

2.3.6 Further Improvement of Sensing Polymers by UV Irradiation

To further improve sensor performance, we subjected the sensing polymers as prepared above to UV irradiation. Figure 11 indicates that the sensor performance can be significantly improved by UV irradiation and the relative resistance changes have been increased by a factor of 3 to 4. Although the detailed mechanism remains unknown, the observed improvement of sensor response could be attributed to the potential changes in functional groups or the number of cross linking of the sensing polymer.

2.4 Headspace VOC Detection Using Chemiresistor Array

In this section, we systematically evaluate the potential applications of a sensor array in headspace VOC detection. We focus on the following specific issues:

- For a single-component system, can the sensor array correctly identify the chemical compound and quantify its concentration?
- If the chemical compound is not in the list of VOCs used for sensor training, can the sensor array provide sufficient information about the chemical characteristics of the compound for further determination?
- To what extent can the sensor array differentiate individual VOCs in a multi-component system?

2.4.1 Testing Procedure

As discussed in Section 2.3.2, five polymers were finally selected to form a chemiresistor array: Ethylene/Vinyl acetate copolymer (PEVA), Polystyrene (PS), Styrene/ Ethylene-Butylene, ABA copolymer (ScEB), Vinyl chloride/Vinyl acetate/Hydroxypropyl acrylate terpolymer (VCVAHPA), and Zein. The sensing polymer composites were prepared as described in Section 2.3. 0.08 gram of each polymer was mixed with 0.02g carbon black (XE2, Degussa,) in the appropriate solvent, followed by ultrasonication for three minutes. The mixtures were then freeze deposited in replicates onto five chips with each containing four deposits (Table 4). Six VOCs were tested: 1,1,1-trichloroethane (TCA), trichloroethylene (TCE), carbon tetrachloride (C), chlorobenzene (B), Toluene, methylene chloride (D). which are a subset of VOCs that are required to be quantified in transuranic waste characterization (See Table 1).

The chips were then mounted on the 16-pin dual inline package (DIP). For easy operations, the DIP was inserted in an “a” socket, which was wire-connected with the HP data acquisition. The “a” socket was housed in a custom-designed force-flow chamber with the deposited side inwards to the chamber. The chemiresistor was equilibrated with dry nitrogen gas overnight. The concentration of VOC was controlled by a bubbling system. 150 mL of the liquid VOC was added to a bubbler. For a 6-VOC mixture, 25 mL of each VOC liquid was added in the bubbler, making a total volume of 150 mL. Nitrogen gas was lined to the bottom of the bubbler to force a VOC flow out of the bubbler through a porous glass-fritter. The VOC vapor was carried by nitrogen gas and mixed with the auxiliary nitrogen gas before reaching the forced-flow chamber. The ratio of VOC to N_2 was controlled by a valve system. The gas chamber was

purged by a VOC/N_2 mixture for 5 minutes and then only N_2. The gas purging cycle was repeated five times for one VOC or six-VOC tests. For two-VOC tests, two bubblers were used to provide separate VOC flows, which were then mixed with N_2 gas at desired ratios (usually, 3, 5, or 10 %).

Table 4. Sensor array for VOC detection

Chip #	Polymer in the polymer-carbon black composite
1	PEVA, PS, ScEB, VAVAHPA
2	PEVA, PS, ScEB, VAVAHPA
3	PEVA, ScEB, VAVAHPA, Zein
4	PEVA, ScEB, VAVAHPA, Zein
5	PS, PS, Zein, Zein

2.4.2 Results

The relative resistance change ($\Delta R/R_b$) of each sensing polymers in response to individual VOCs are shown in Figure 14 and Table 5. As shown in Table 5, over the concentration ranges tested, most sensing polymers have nearly linear responses to VOC concentration changes. However, the linear regression lines do not pass through the original coordinate (i.e., $\Delta R/R_b$ 0 for the absence of VOC), indicating that the sensor responses may not be linear over a whole VOC concentration range. The behavior of sensing polymer Zein is more complicated, and its responses to TCE, CCl_4, and toluene are not linear, or even not monotonic. However, notice that the overall relative resistance changes of this polymer are small, probably within the range of measurement errors. The lack of responses of polymer Zein to TCE, CCl_4, and toluene may provide additional information for the sensor array to discriminate these VOCs from others. It can be seen in Figure 14 that the slopes of the response of a given polymer vary from VOC to VOC. These variations constitute a basis for the sensor array to differentiate different VOCs

Figure 15 and Table 6 summarize the responses of the sensor array to binary VOC mixtures as well as six-VOC mixtures. The response patterns are similar to the single-component systems, with the PEVA having the highest sensitivity and the Zein being the least responsive.

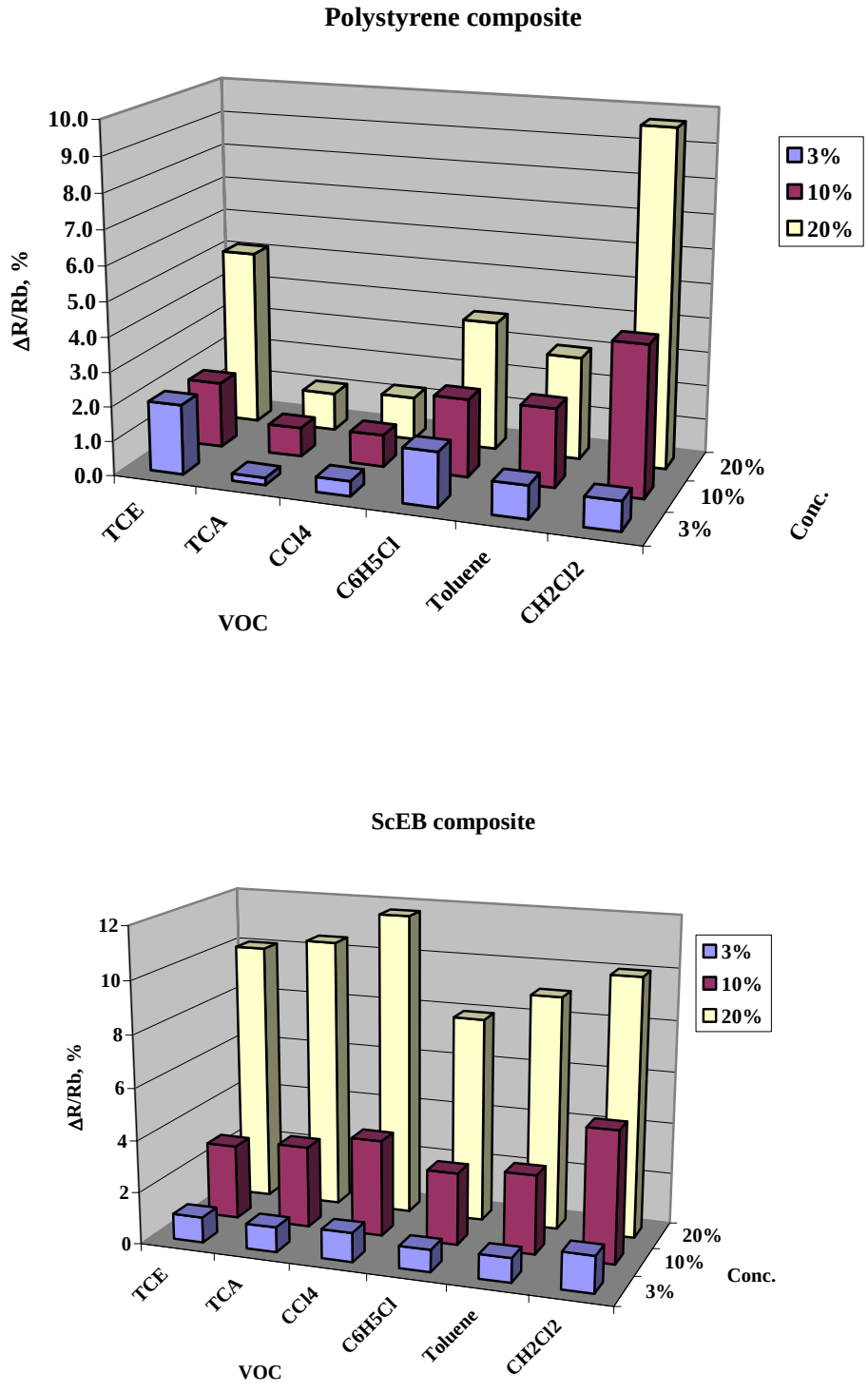

Figure 14. Relative resistance changes of sensing polymers responding to individual VOCs. VOC concentrations are referred to the percentages of saturated VOC vapor concentrations.

Table 5. Relative resistance changes of sensing polymer responding to varying VOC concentrations. Each tabulated value is the average of eight replicates.

	VOC concentration in nitrogen gas					
PEVA	**3%**	**10%**	**20%**	**Slope**	**Intercept**	**Correlation coefficient**
TCE	2.0	9.6	30.1	168.2010	-4.6052	0.9880
TCA	1.7	6.9	23.8	132.7954	-3.8233	0.9816
CCl4	1.5	6.4	23.8	133.8636	-3.8233	0.9775
C6H5Cl	1.3	8.6	19.4	106.4227	-1.9629	1.0000
Toluene	1.4	5.9	17.9	98.8503	-2.4848	0.9879
CH2Cl2	5.2	19.1	44.2	230.9673	-2.5728	0.9981
PS						
TCE	2.02	1.91	5.14	19.3434	0.89612	0.8997
TCA	0.21	0.84	1.11	5.0955	0.15998	0.9437
CCl_4	0.43	0.92	1.26	4.7525	0.34784	0.9780
C_6H_5Cl	1.57	2.25	3.76	13.0480	1.09422	0.9934
Toluene	0.95	2.27	2.99	11.6665	0.78768	0.9634
CH_2Cl_2	0.84	4.33 (5% conc.)	9.69 (20% conc.)	122.7308	-2.41051	0.9927
ScEB						
TCE	0.98	2.88	10.06	54.6640	-1.3707	0.9753
TCA	0.96	3.15	10.49	57.2394	-1.4335	0.9799
CCl4	1.12	3.71	11.69	63.4115	-1.4666	0.9880
C6H5Cl	0.85	2.78	7.93	42.3264	-0.8007	0.9880
Toluene	0.93	3.04	9.02	48.4527	-0.9992	0.9860
CH2Cl2	1.40	5.05	10.00	50.5331	-0.0753	0.9999
VCVAHPA						
TCE	1.21	0.85	3.08	11.7727	0.4171	0.8420
TCA	0.18	0.33	0.63	2.6349	0.0896	0.9966
CCl4	0.16	0.47	0.67	2.9211	0.1115	0.9712
C6H5Cl	0.93	0.89	3.02	12.8816	0.1982	0.9055
Toluene	0.92	0.90	2.65	10.6837	0.3120	0.9081
CH2Cl2	1.09	2.44	5.24	24.6808	0.2118	0.9953
Zein						
TCE	0.74	1.83	1.46	3.6518	0.9424	0.5624
TCA	0.11	0.20	0.19	0.4400	0.1193	0.9689
CCl4	0.00	0.51	0.18	0.7914	0.1437	0.2632
C6H5Cl	0.23	0.81	0.55	1.5792	0.3586	0.4631
Toluene	0.14	0.64	0.37	1.0910	0.2654	0.3707
CH2Cl2	2.15	3.65	4.24	11.8748	2.0392	0.9401

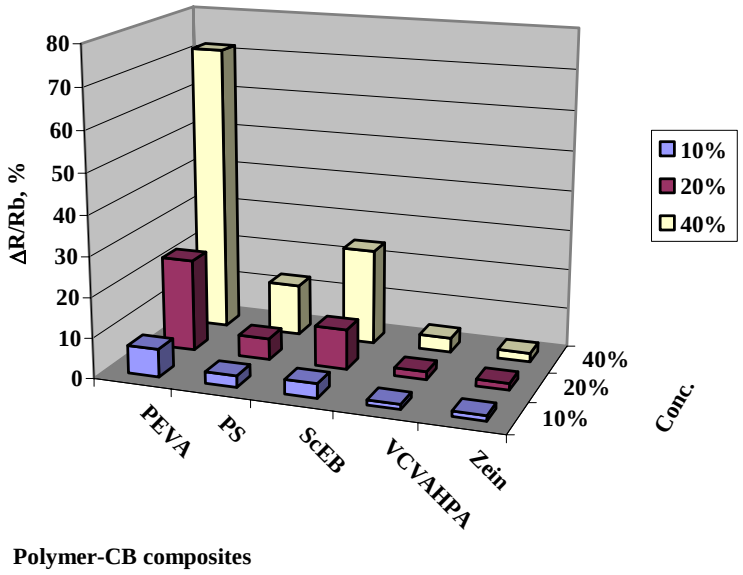

Figure 15. Relative resistance changes of sensing polymers responding to the mixture of all six VOCs.

Table 6. PEVA responses to binary VOC combinations

Combination of polymers	Concentrations			
	10/10	**10/5**	**5/10**	**5/5**
AC	18.2		12.4	
AD	31.5			11.1
AB	21.7		14.4	
AE	30.3			21.5
AT	23.8	17.4		
CD	37.8	17.9		
CB	21.5		14.0	
CE	30.8	20.7		
CT	20.5		14.3	
DB	24.5		13.0	
DE	37.6			13.3
DT	36.0		11.3	
BE	22.3	11.7		
BT	21.7	14.4		
ET	17.5		12.0	

A – TCA, B- chlorobenzne, C – carbon tetrachloride, D – methylene chloride, E – TCE, T- toluene

2.4.3 Discussions

An ideal approach to chemical sensors is made use of a so-called "lock-and-key" design, where a specific receptor is synthesized to have a high selectivity for the analyte of interest. This approach requires the synthesis of a separate, highly selective sensor for each analyte to be detected in the controlled background. This generally poses a challenging problem in synthesizing sensing materials. An alternative approach is to design an array with every element in the chosen to respond to a number of different chemicals or classes of chemicals (Albert et al., 2000). Although in this design identification of an analyte cannot be accomplished from the response of a single-sensor element, a distinct pattern of responses produced over the collection of sensors in the array could provide a "fingerprint" that would allow classification and identification of the analyte. The advantage of this approach is that it can yield responses to different analytes, including those for which the array was not originally designed. In this section, we apply this concept to the headspace gas detection in radioactive waste characterization, based on the testing data summarized in the previous section.

Use of a microsensor array to determine total VOC concentrations: One of the issues generally encountered in waste characterization is whether the total VOC concentration in a specific waste container exceeds a specified limit so that comprehensive headspace gas sampling and analysis are required. Figure 16 shows that a microsensor array with two or more chemiresistors is able to differentiate waste containers against a specified total VOC concentration limit. Therefore, it is feasible to use of microsensors as a screening tool to reduce the headspace gas sampling rates in the existing waste characterization practice. The reduction in headspace gas sampling rate can lead to a significant cost saving.

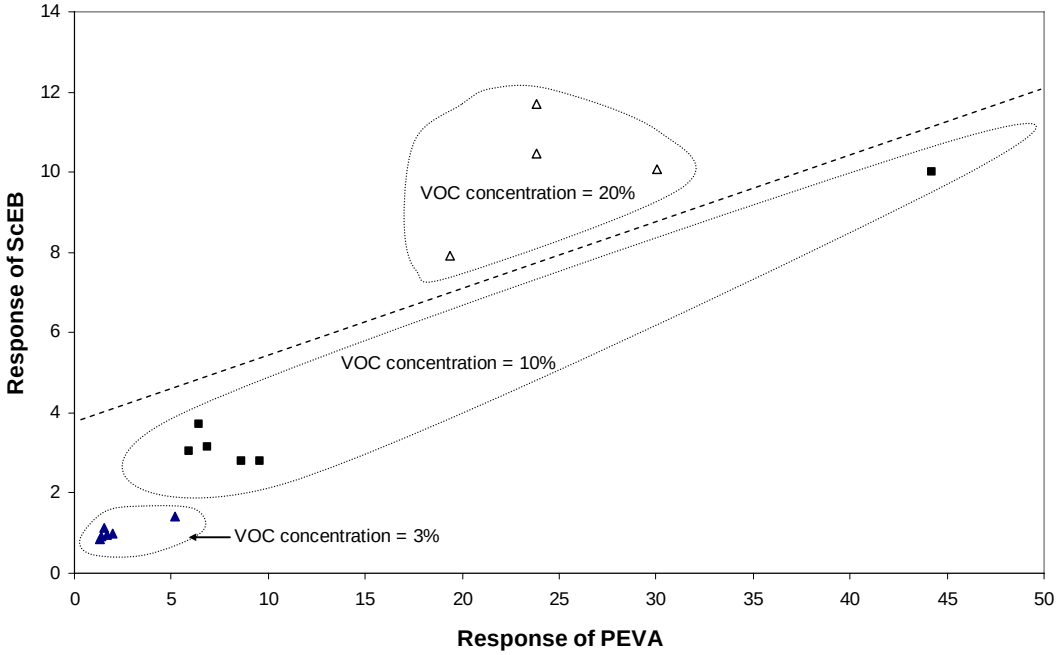

Figure 16. Discrimination of gas samples for their total VOC concentrations using two chemiresistors. The dashed line is a hypothetical total VOC concentration limit.

Identification of a VOC from a known candidate list: Assuming that we have a prior knowledge that a waste container to be characterized is dominated by a single VOC in the headspace gas and this VOC is among the list used for sensor training, we now want to identify what VOC is actually present in the headspace. For this case, the identification of VOC is rather straightforward. From a data set used for sensor training, we can constrain the response of each chemiresistor to each individual VOC (R_{ij}) as a function of VOC concentration (C_j):

$$R_{ij} = f_i(C_j) \quad \text{for } i = 1, 2, \ldots, \text{m}; j = 1, 2, \ldots, \text{n} \tag{2}$$

where m and n are the number of chemiresistors in the sensor array and the number of VOCs in the training data set, respectively. The VOC can then be identified as the one (subscripted by *j*) for which all sensors can provide a consistent prediction of the concentration:

$$\underset{j}{\text{Minimum}} \quad \sigma\left\{f_1^{-1}(R_{1j}), \quad f_2^{-1}(R_{2j}), \quad ..., \quad f_{n1}^{-1}(R_{nj})\right\} \tag{3}$$

$$C_j = \text{mean} \quad \left\{f_1^{-1}(R_{1j}), \quad f_2^{-1}(R_{2j}), \quad ..., \quad f_{n1}^{-1}(R_{nj})\right\} \tag{4}$$

where is the standard deviation. Using linear functional dependences constrained in Table 5, we have applied the above equations to the data listed in the table. The sensor array has correctly identified VOCs in these samples at a rate of 78% (Table 7). The errors with the prediction of VOC concentrations are less than 73%. The polymers that give the best concentration prediction are also listed in Table 7. We expect that the sensor performance can be improved by using more accurate functional dependences of sensor responses on VOC concentrations.

Table 7. Identification of VOC from a known candidate list

VOC tested	Experimental conc.	Predicted conc.	VOC identified	Polymer that gives the best prediction
TCE	0.03	0.052	v	PEVA
TCE	0.1	0.063	v	PEVA
TCE	0.2	0.22	v	PEVA
TCA	0.03	0.021	v	VCVAHPA
TCA	0.1	0.083	CCl4	VCVAHPA
TCA	0.2	0.19	v	VCVAHPA
CCl_4	0.03	0.029	v	PEVA
CCl_4	0.1	0.1	v	ScEB
CCl_4	0.2	0.2	v	PEVA
C_6H_5Cl	0.03	0.039	TCE	PEVA
C_6H_5Cl	0.1	0.067	TCE	PEVA
C_6H_5Cl	0.2	0.21	v	PEVA
Toluene	0.03	0.037	v	PEVA
Toluene	0.1	0.064	TCE	PEVA
Toluene	0.2	0.19	v	PEVA
CH_2Cl_2	0.03	0.027	v	ScEB
CH_2Cl_2	0.1	0.1	v	PS
CH_2Cl_2	0.2	0.2	v	ScEB

v – correctly identified

Identification of VOC without any prior knowledge: In many cases, we do not have any prior knowledge of whether the targetVOC is among the list of compounds used for sensor training. Therefore, it is desirable that a microsensor array is able to predict not only the concentration of VOC but also certain physiochemical parameters of the VOC that can be used for further identification of the compound. Grate and his colleagues (Grate et al., 1999; Grate et al., 2001) have proposed to use a microsensor array to predict vapor descriptors of volatile organic compounds, using linear solvation energy relationships (McGill et al, 1994; Abraham, et al. 1994; Abraham, et al. 1995). We adopt a similar approach here.

For simplicity, we focus on a low VOC concentration case, where the response of chemiresistor *i* (R_i) to VOC concentration (C) can be described by the following equation:

$$R_i = k_i C \tag{5}$$

where k_i is the proportional constant , which we assume to follow the following linear solvation energy relationship:

$$\log k_i = a_i^0 + a_i^V V + a_i^H \log L_{16} + a_i^W \log L_W \tag{6}$$

where V is the characteristic volume of the VOC; L_{16} is the gas-hexadecane partition coefficient at 298 K; and L_W is the Ostwald solubility coefficient of VOC in water at 298 K. The terms, L_{16} and L_W, in Equation (6) account for the affinities of the VOC to nonpolar organic solvent and polar solvent water, respectively; and the term V accounts for the effect of molecular size on polymer volume expansion due to sorption of VOC. The constants, a_i^0, a_i^V, a_i^H, and a_i^W, in Equation (6) are obtained by a regression analysis of Equations (5) and (6) against a training data set. The values of a_i^0, a_i^V, a_i^H, and a_i^W for the chemiresistors we tested are listed in Table 8. In the regression, only data obtained at low VOC concentrations (3% of saturated vapor concentrations) are used. The values of V, L_{16}, and L_W used in the regression are from Abraham et al. (1994).

Table 8. Regression coefficients a_i^0, a_i^V, a_i^H, and a_i^W obtained for chemiresistors tested

	a_i^0	a_i^V	a_i^H	a_i^W	R
PEVA	2.85101	-0.99446	-0.13518	0.164335	0.994809
PS	1.248213	-5.59464	1.451488	0.054224	0.890331
ScEB	1.930449	-0.26434	-0.07004	0.005041	0.945455
VCVAHPA	1.026007	-3.09846	0.770045	0.5704	0.867427
Zein	3.495444	-7.48581	1.049917	-0.05561	0.972764

After the determination of a_i^0, a_i^V, a_i^H, and a_i^W, Equations (5) and (6) can be rearranged into:

$$a_i^V V + a_i^H \log L_{16} + a_i^W \log L_W + \log C = \log R_i - a_i^0 . \quad (7)$$

For a given set of sensor array responses, both the concentration (C) and solvation parameters (V, L_{16}, and L_W) can be solved simultaneously by a inverse least square analysis. Up to date, solvation parameters have been tabulated for some 2000 compounds (e.g., Abraham, et al. 1994). Therefore, it is possible to use the solvation parameter values determined from Equation (7) to identify an unknown VOC by matching the values with those tabulated.

We have applied Equation (7) back to the training data set. The results are shown in Table 9. It can be seen in the table that model predictions are in good agreement with experimental data, especially for the VOC concentration, the characteristic volume of VOC, and the the gas-hexadecane partition coefficient. The relatively large error associated with L_W might result from the lack of representative VOCs in the training data to capture a wide range of variability in L_W.

Table 9. Comparison of model-predicted concentrations and solvation parameters with experimental data

	C exp.	C predicted	V	V predicted	log L_{16}	log L_{16} predicted	log L_w	log L_w predicted
TCE	0.03	0.029	0.7146	0.7134	2.997	3.130	0.32	0.69
TCA	0.03	0.028	0.7576	0.7580	2.733	2.652	0.14	0.16
C_6H_5Cl	0.03	0.030	0.8388	0.8397	3.657	3.541	0.82	0.61
Toluene	0.03	0.031	0.8573	0.8565	3.325	3.438	0.65	0.78
CH_2Cl_2	0.03	0.030	0.4943	0.4944	2.019	2.007	0.96	0.91

The modeling approach developed above can in principle be extended to high VOC concentration cases. However, this requires that the functional dependence of chemiresistor response on VOC concentration (Eqn. 2) is well constrained and all coefficients in the function can be correlated to certain known physical/chemical parameters of VOCs. For a sensor array to have a robust performance, it is required that

Number of chemiresistors in the sensor array
$\geq$ number of solvation parameters to be quantified + 1 (8)

Our work has shown that the minimum number of chemiresistor required for detection an unknown VOC in a single-component system is four.

Identification of VOCs in multcomponent systems: Equations (5) and (6) can be extended to a muticomponent system:

$$R_i = \sum_{j=1}^{n} C_j e^{a_i^0 + a_i^V V + a_i^H \log L_{16} + a_i^W \log L_W} \quad (9)$$

where *n* is the number of VOCs in the system. To effectively constrain the concentration of each VOC and the related solvation energy parameters, it is required that:

Number of chemiresistors in the sensor array
≥ (number of solvation parameters to be quantified + 1) x number of VOCs (10)

For instance, to detect VOCs in a ternary system, a sensor array needs to contain at least 12 chemiresistors. This number increases rapidly with the number of VOCs involved. In many cases, however, we even do not know how many VOCs are actually present in the system. Therefore, use of Equation (9) to determine unknown VOCs in a general multicomponent system may not be practical. Since we have demonstrated the capability of a sensor array for identifying an unknown VOC in a single component system, we suggest that a most feasible way to analyze a complex VOC mixture using a sensor array would be to combine a chromatographic separation with sensor array detections. A similar approach has been proposed by Lu and Zellers (2002).

3. Development of Preconcentrator for VOC Detection

3.1 Overview of Preconcentrators

Despite the apparent usefulness of the chemiresistor for many environmental applications, some concern has been expressed over the sensor's lack of sensitivity for particular analytes in low concentrations (see Table 1). In general, a chemiresistor polymer optimally paired with a given analyte of interest can detect approximately $1/1000^{th}$ of the analyte vapor pressure. For compounds with high vapor pressures and low desired detection limits, this may not result in favorable detection capabilities of the simple chemiresistor. For example, carbon tetrachloride, with a vapor pressure of 91.3 torr at 20°C, would be detectable by a chemiresistor at approximately 120 ppm; however, OSHA has a proposed time-weighted average exposure limit for carbon tetrachloride at 2 ppm. Clearly, an improvement in detection limits would be necessary for the chemiresistor to be useful in this application.

To address the issue of lowering chemiresistor detection limits, work has been performed on coupling a microfabricated planar preconcentrator with the chemiresistor. The preconcentrator consists of a thin film of absorbent material deposited on a resistive wire trace. The absorbent film allows for reversible accumulation of chemical vapors over a period of time until heated by running current through the wire trace. When the absorbent material is heated, the absorbed VOCs are thermally desorbed and can be directed as a concentrated plume to a detection system. Thus, the preconcentrator serves as a simple method for collecting and concentrating VOCs in a sensing system for a prescribed period of time. The combination of the sensor response signal and knowledge of the specified integration period allows derivation of an average analyte concentration during the VOC accumulation period. Enhanced detection was demonstrated through the use of the hybrid chemiresistor/preconcentrator, but design issues still needed to be addressed to optimize performance of the hybrid. For this reason our research has progressed along a two-fold path with one group investigating characteristic sensitivity, selectivity and repeatability of the hybrid unit in its current configuration while another undertook two-piece testing that allowed for optimization of geometry, spacing, load time and other parameters. Results of each group are reported in this section.

3.2 Fabrication of Preconcentrators

The fabrication of the micro-hotplate preconcentrator (Manginell et al., 2000) utilized a KOH-etched 4 inch wafer (yield ~200 hot-plates) with a silicon nitride coating. The KOH-etching produces a 1-micron thick silicon nitride membrane, which has a very low thermal mass. A binding agent was created by mixing 0.5% Polyisobutylene (0.92 g/ml PIB) in 1 ml of TCE (1.4642 g/ml TCE) by mass. This binding agent was then deposited onto the hot-plate with 65m x 510m x ~5' of High Pressure PEEK tubing (Upchurch, P/N 1543) in combination with 10-32 female-female LUER, Teezel (Upchurch, P/N P-659) and BD 10ml Syringe, LUER-LOK™ Latex Free (Upchurch, P/N B-310). Two different applications were used. In some cases the binding agent was spread over the total surface of the silicon nitride membrane and in others one dot of binding agent was applied to the surface of the silicon nitride membrane. Carboxen 1003 40/60 mesh (Supelco, P/N 10471) was ball milled to 325 mesh and was deposited on top of the

binding agent (Figure 17). The preconcentrators were then placed in an oven at ~100ºC for 1-2 hours to allow for the adhesion of Carboxen 1003 to the polymer binding agent. (17). Wires were then soldered to the preconcentrator utilizing a solder (62% Tin, 36% Lead, 2% Silver) with a melting point of 179ºC (350ºF). This solder allows for a smooth and consistent flow of solder onto the platinum pads. A smooth and consistent solder flow is very important to avoid a weak/cold solder joint which could lead to erratic and inconsistent readings, or a lack of heating voltage being applied.

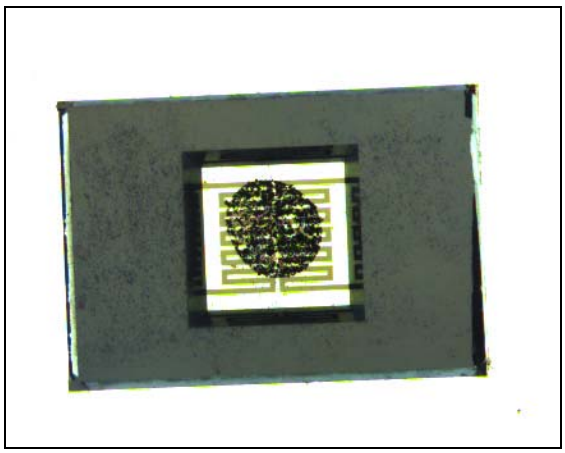

Figure 17. Preconcentrator with Polymer and Carboxen 1003.

3.3 Preconcentrator Heating Tests

Tests were conducted on the preconcentrator to identify the temperature response, linearity, and stability, as well as to identify the actual temperature achieved when 5 volts was applied for a prescribed duration. Four preconcentrators and a T-Type thermocouple were placed in an oven. The oven was set to ~110ºC and allowed to stabilize. The oven was then turned off and permitted to drop to room temperature (~23ºC). During this process the resistance of the preconcentrator and the thermocouple was monitored using the Agilent 34970A datalogger. The associated data was collected and plotted using Microsoft® Excel 2000. The resistance was plotted as a function of temperature recorded by the T-Type thermocouple to establish a calibration curve. As can be seen in Figure 18 the preconcentrator responds to temperature in a linear manner.

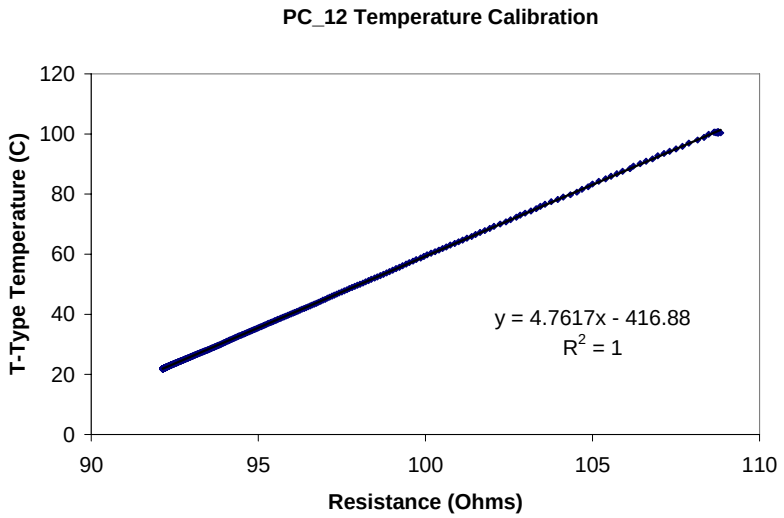

Figure 18. Dependence of preconcentrator resistance on temperature.

The preconcentrators were then connected to a power supply that was adjusted to supply 5 volts for 10 seconds. The resistance value was calculated from the measured current and voltage utilizing Ohms Law and then plugged into the temperature-calibration curve fit to calculate the temperature of the preconcentrator under energized conditions. Figure 19 shows all four preconcentrator temperatures as a function of time before, during, and after the heating. All four reach a temperature of ~300ºC very rapidly and are fairly steady. After the power supply was turned off, the preconcentrator temperature dropped back down to ambient temperatures very quickly.

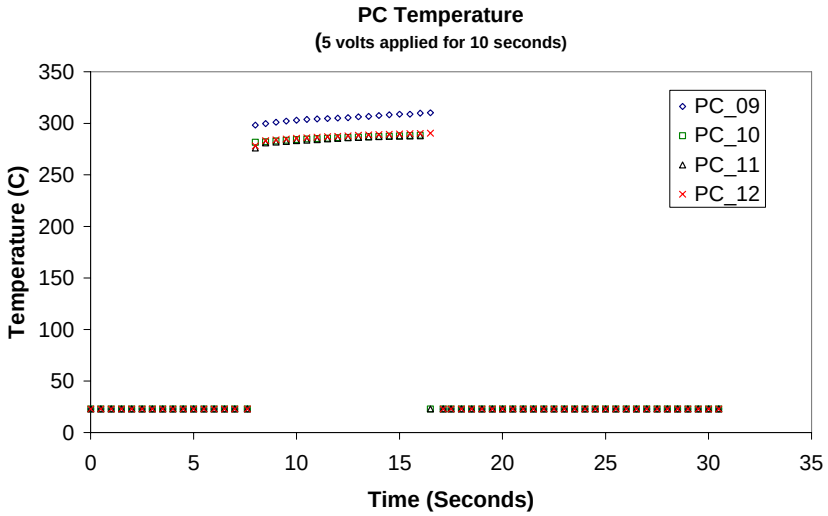

Figure 19. Preconcentrator temperature as a function of time before, during, and after heating.

3.3.1 Two-Piece Preconcentrator/Chemiresistor Testing

Tests were conducted to determine the response of a chemiresistor sensor to m-xylene with and without preconcentration. Results have showed that by adding a microfabricated preconcentrator to a chemiresistor sensor, detection limits of m-xylene were decreased by more than two orders of magnitude, from 13.5 ppm to 61.8 ppb, without significantly increasing the complexity of the sensing system.

Controlled chemical exposures were performed through the use of custom gas cylinders of m-xylene with analytically verified concentrations or gas-washing bottles filled with liquid m-xylene. A range of concentrations were generated by diluting and controlling gas flows through a series of valves (SMC solenoid valve NVZ110 and Nupro/Swagelok stainless bellows valve SS-4BK-1C) and mass flow controllers (Brooks Instrument 5850E mass flow controllers) operated through a LabVIEW interface on a Macintosh computer. Analyte concentration levels were confirmed through the use of a RAE Systems ToxiRAE or ppbRAE photo-ionization detector. The chemiresistor sensor (A64) used in this study consisted of a four-chemiresistor array on a single silicon substrate with integrated on-chip platinum-wire temperature sensor and resistive heater bars for temperature control. Arrays are packaged in a 16-pin DIP for ease of electrical connections. Chemiresistor polymer solution preparation involves dissolving the polymer in a solvent and adding 40% by weight of 20-30 nm graphitized carbon particles. The polymer solution is subjected to sonication from a point ultrasonic source to enhance ink uniformity, using 15 half-second pulses separated by one-second rest periods. Solution deposition on the sensor silicon substrate is performed with an Asymtek Century Series C-708 automated fluid dispensing system.

Preconcentrator devices were fabricated on a Bosch-etched silicon wafer, with platinum-wire heating elements supported by a thin silicon nitride membrane. A solid analyte-absorbent phase was dispersed in a thin dissolved polymer film used strictly for phase adhesion to the substrate. Individual preconcentrator substrates were also packaged in a 16-pin DIP for ease of electrical connections. Voltage pulses that were applied to heat the preconcentrator were controlled through manual triggering of a Systron Donner Model PLS 50-1 precision power supply. Two 16-pin DIPs were used to separately package the chemiresistor and the preconcentrator. The two DIPs were placed in a face-to-face orientation to allow only a short vertical distance between the chemiresistor and the preconcentrator. Figure 20 shows the custom housing designed for mating the two 16-pin DIPs in the lab.

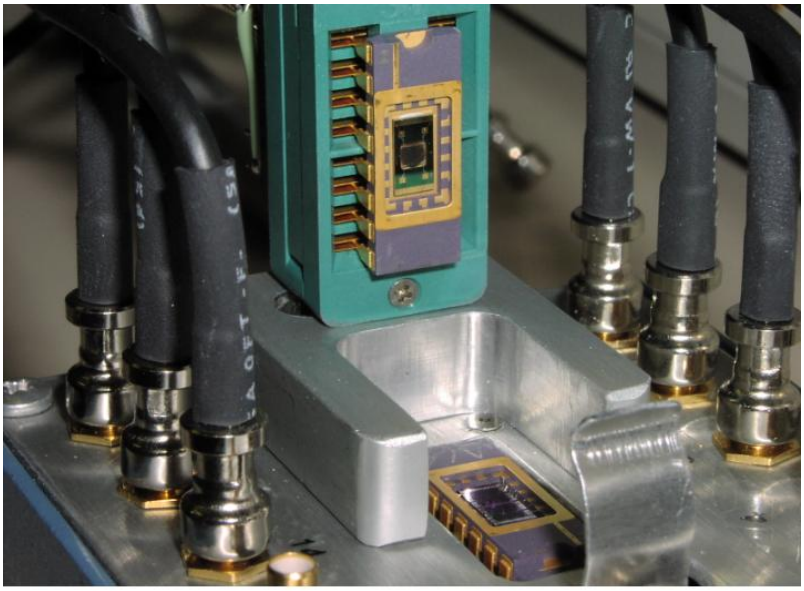

Figure 20. Custom housing designed for mating the two 16-pin DIPs in the lab. Both the chemiresistor die and preconcentrator die are packaged individually in 16-pin DIPs.

3.3.2 Testing Results

In the two piece preconcentrator/chemiresistor test, we focused on the detection of m-xylene using PEVA as a sensing polymer. Commercially available preconcentrator phases were considered for use based on temperatures of absorption and desorption that would be consistent with environmental monitoring scenarios for analyte loading (~30°C under elevated temperature conditions to prevent moisture condensation on the sensor) and the typical temperature attained by the preconcentrator for analyte thermal desorption (300°C in less than 1 millisecond, due to the small thermal mass of the silicon nitride membrane on the hotplate).

Selection of Preconcentrator Phases: From our initial screening, five preconcentrator phases were identified for further study: Carbosieve, Carbotrap, Carboxen 569, Carboxen 1000, and Tenax GR. Each phase was prepared on an individual preconcentrator device and exposed to a flowing stream of 0.2% saturated vapor pressure of m-xylene (~21 ppm) for a five-minute period. Subsequent to loading the preconcentrator phase with m-xylene, the devices were mated face-to-face with the chemiresistor using the custom housing, and pulsed with five volts for five seconds. The magnitude of response of the chemiresistor sensor to all five phases, represented as an increase in chemiresistor resistance relative to the initial baseline resistance ($\Delta R/R_b$, %), is shown in Figure 21. As clearly shown, the Carboxen 1000 phase outperforms all other preconcentrator phases for preconcentration of m-xylene, with an average $\Delta R/R_b$ of 143%, more than five-times the signal provided by any other preconcentratior phase. Carboxen 1000 was therefore selected for continued performance assessment.

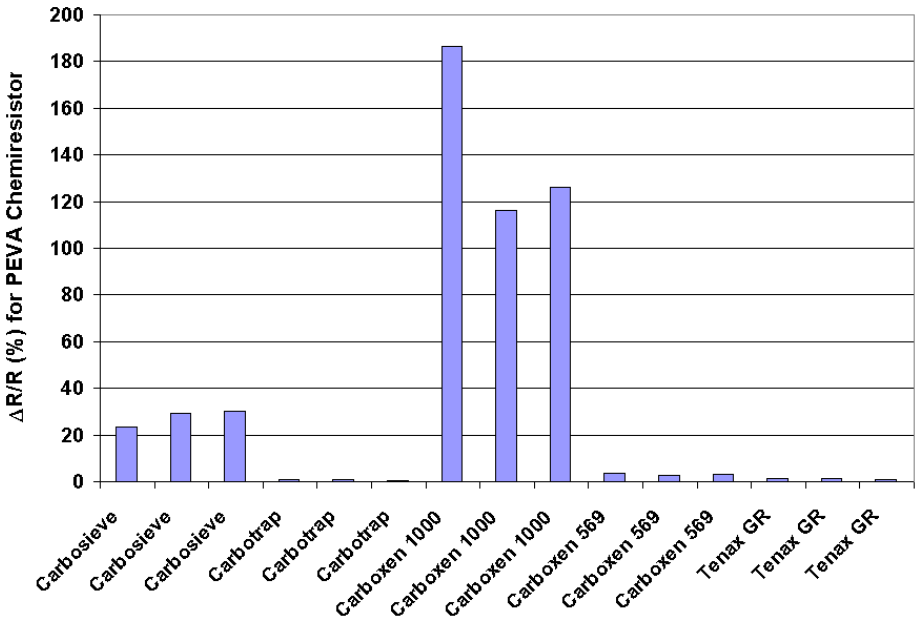

Figure 21. Responses of PEVA chemiresistor to m-xylene vapor for different preconcentrator phases.

Enhancement of chemiresistor detection limits: In order to assess the performance improvement provided by a preconcentrator, a study of the detection limit for the unaided chemiresistor sensor was performed. As mentioned previously, we had predicted the capability of chemiresistors to detect an analyte to be as low as 0.1% of the saturated vapor pressure. The noise threshold of the sensor was estimated to be equal to three times the standard deviation (σ_{Rb}) of the sensor response during quiescent, unexposed (no chemical), ambient conditions. This value was then divided by the average baseline resistance ($R_{b,avg}$) during the quiescent period to yield the relative change in resistance ($3\sigma_{Rb}/R_{b,avg}$) that corresponds to a minimum detection limit above the noise threshold. For the PEVA chemiresistor used in the experiments, $3\sigma_{Rb}/R_{b,avg} = 0.249\%$. The polynomial fit to calibration data (Figure 22) allows determination of a limit of detection of 13.5 ppm. This detection limit of 13.5 ppm corresponds to slightly less than 0.12% of the saturated vapor pressure of m-xylene (11,600 ppm under our typical laboratory conditions).

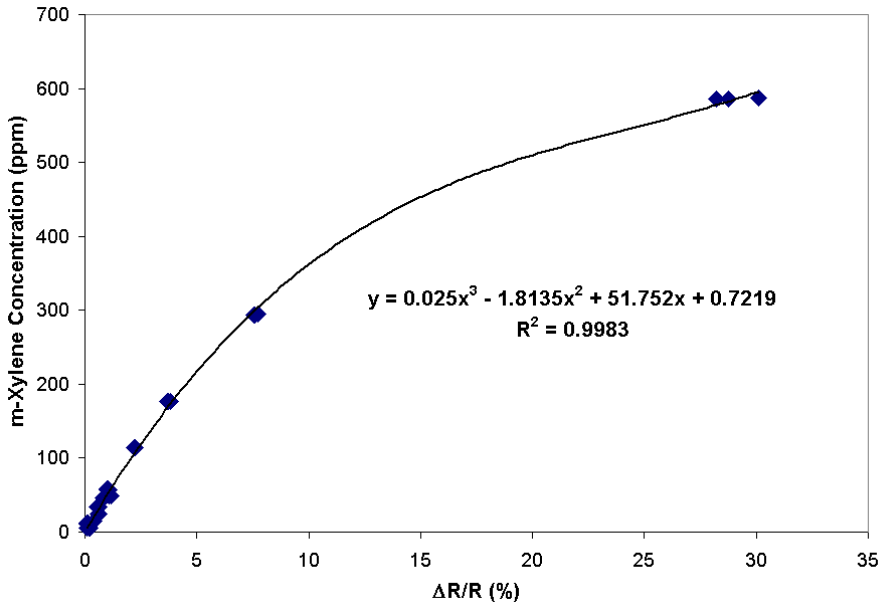

Figure 22. Calibration curve for the unaided (no preconcentrator used) PEVA chemiresistor A64 in response to m-xylene vapor.

To assess the improvement in detection limits provided by preconcentration, the Carboxen 1000 preconcentrator was exposed to a series of low concentration m-xylene streams. When using the chemiresistor to detect extremely low concentrations of m-xylene through the assistance of a preconcentrator, as in this case, the thermal expansion of the PEVA polymer due to the heating of the preconcentrator device must be taken into consideration to avoid confusion with swelling caused by the presence of the analyte. At the very low concentrations involved in a detection limit study, this is especially important, as the temperature response of the chemiresistor begins to be on the order of the analyte response of the chemiresistor. The necessary correction was accomplished by subtracting the response of the chemiresistor to an average blank heat pulse (no absorbed analyte) from the response of the chemiresistor to a corresponding analyte-loaded pulse. Both the analyte-loaded pulse and the blank heat pulse are calculated as individual $\Delta R/R_b$ values, each with its respective baseline resistance value (to keep consistent with changes in ambient conditions that can impact the baseline), and simple subtraction of one value from the other correctly accounts for the temperature rise associated with the heat pulse.

Applying similar logic to that previously used on the unaided chemiresistor, a detection limit is conceptually defined as a sensor signal that can be differentiated above the signal noise, quantitatively seen as a signal greater than or equal to three standard deviations above the mean noise level. However, in this instance, the sensor signal, an analyte-loaded pulse, must be differentiated from the blank heat pulses, so the mean and standard deviation for the limit of detection are in reference to the set of blank heat pulse $\Delta R/R_b$ values, and not to simple resistance values. As temperature correction must still be applied to remove the influence of the

heat pulse, the sensor response corresponding to the limit of detection is calculated as the three standard deviations above the mean blank heat pulse, corrected by the mean blank heat pulse. The equation can be written as follows:

$$\left[\left(\frac{\Delta R}{R_b}\right)_{\text{avg heat pulse}} + 3\sigma_{\text{avg heat pulse}}\right] - \left(\frac{\Delta R}{R_b}\right)_{\text{avg heat pulse}} = 3\sigma_{\text{avg heat pulse}} \qquad (11)$$

For the combination of the Carboxen 1000 preconcentrator and the PEVA-40-C chemiresistor, $3\sigma_{\text{avg heat pulse}}$ = 0.153%. Using the polynomial fit to data for preconcentrator exposures over a range of 0 to 2500 ppb (with an R-squared value of 0.9946), the limit of detection at three standard deviations above the mean is 61.8 ppb (Figure 23). Comparing both detection limits at three standard deviations above the mean, preconcentration of m-xylene therefore decreased the detection limit to less than 1/200th of the limit without preconcentration, an improvement of more than two orders of magnitude.

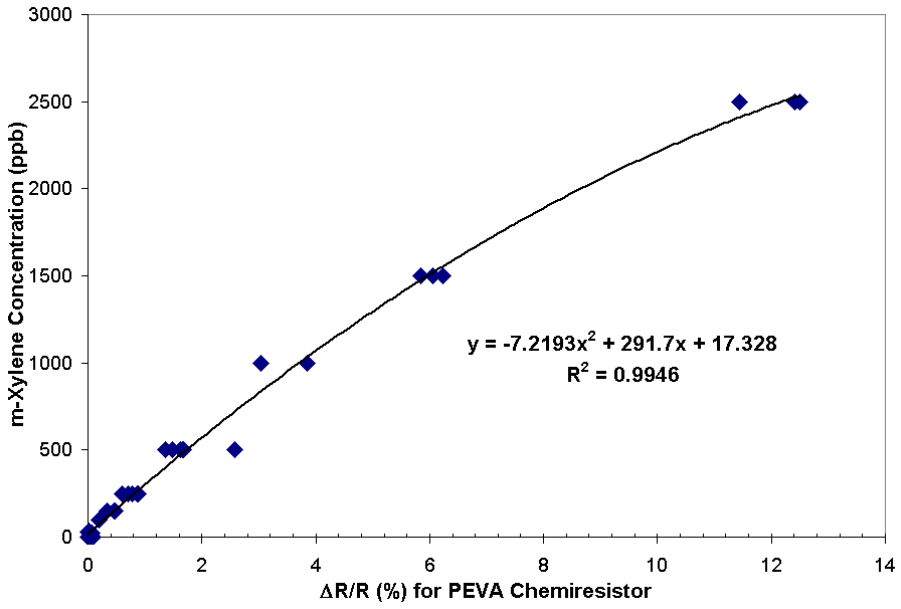

Figure 23. m-Xylene calibration curve for a PEVA chemiresistor coupled with a Carboxen 1000 preconcentrator. Each m-xylene exposure was for five minutes, followed by a five second, five volt pulse to the preconcentrator.

Chemiresistor/Preconcentrator geometry testing: In a practical application, it would prove difficult to remove a preconcentrator for exposure and then replace it in its face to face orientation over the chemiresistor array without incorporating more complexity into the system. The tests were preformed by simply clipping the preconcentrators DIP package face to face with the chemiresistors DIP. The chemiresistor was plugged into a socket with a ribbon cable

attached that allowed the whole package to be suspended in a 1 liter Teflon can with a sealed top. Two extra wires from the ribbon cable were attached to the appropriate pins of the preconcentrator for heating. The Teflon can used ¼ inch Teflon tubing to bring in the dilute gas mixtures from the gas test bed and exhaust it into the hood.

The results of these tests have shown an expected attenuation of signal response for a given exposure time compared with tests where the gas stream was flowing directly over the preconcentrator. Under these more realistic conditions, it seems that diffusion limitations slowed the adsorbtion rate. For exposure times < 1 hour this attenuation is approximately 50%. As exposure times get longer diffusion limitations become less important and eventually the attenuation disappears.

Note that this face-to-face configuration provides the minimum separation achievable when using DIP packages. The die face of the preconcentrator and the sensor array are .038 inch below the top surface of the DIP. Total separation then is .076 inch. Also, note that there is no specific vent window designed for analyte to readily migrate to the preconcentrator. The obvious question is whether an additional vent window can improve the performance of the preconcentrator. To test the effect of a vent window shims were placed between the preconcentrator and the chemiresistor array (Figure 24). The shims were in a "U" shape so they went around 3 sides of the package well and the fourth side was left open. Shims of .0015, .004, .010, and .020 inch were tested with a concentration of 1.5 ppm Xylene for exposure times from 10 minutes to 3 hours.

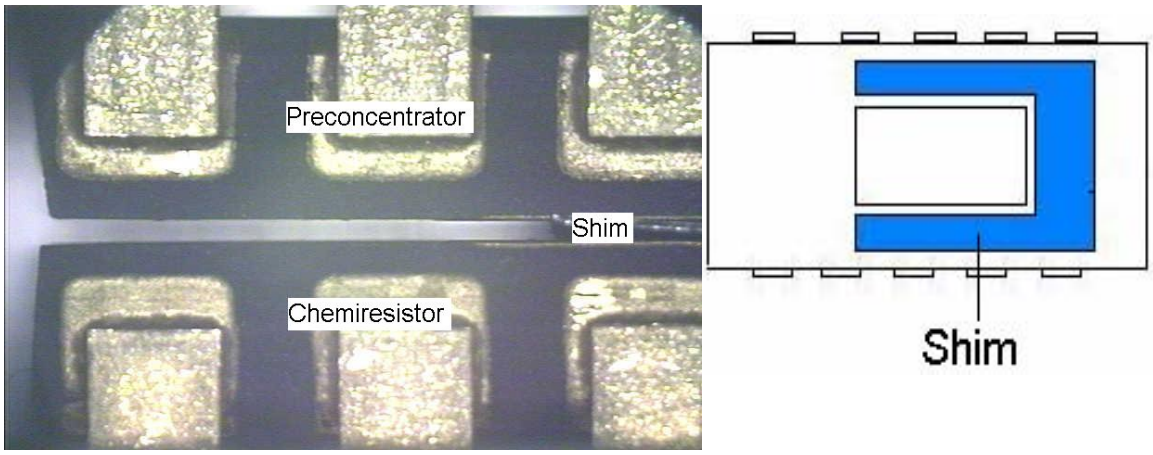

Figure 24. The preconcentrator-chemiresitor configuration for testing the effect of vent window

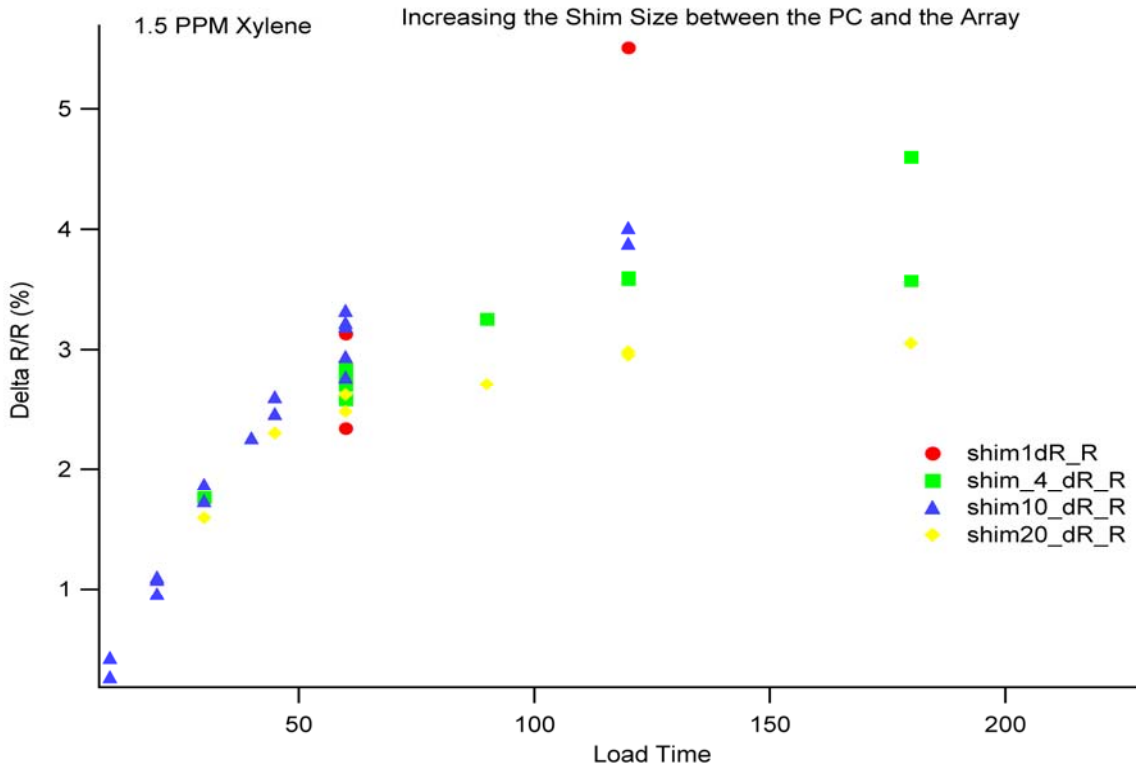

Figure 25. Effect of vent window on the performance of preconcentrator and chemiresistor

The testing results indicate that, as the window gets larger, the response signal of the chemiresistor falls off (Figure 25). This is either because the plume escapes before the sensor can respond to it or because the distance between the sensor and the preconcentrator has become too great for analyte to reach the surface of the chemiresistor.

Using the clipped preconcentrator/chemiresistor assembly with a 0.010-inch shim, a series of exposures were made at decreasing concentrations to find the practical lower concentration detection limits for this sensor system. Exposures of various times were made at 1.5 ppm, 1.0 ppm, 500 ppb and 250 ppb. A rigorous treatment of absolute limit of detection with standard deviation correction for signal and noise over the spectrum of exposures and times is beyond the scope of this work. However, the representative plot included here has clearly demonstrated that if accumulation times are on the order of hours 250 PPB is easily distinguishable (Figure 26).

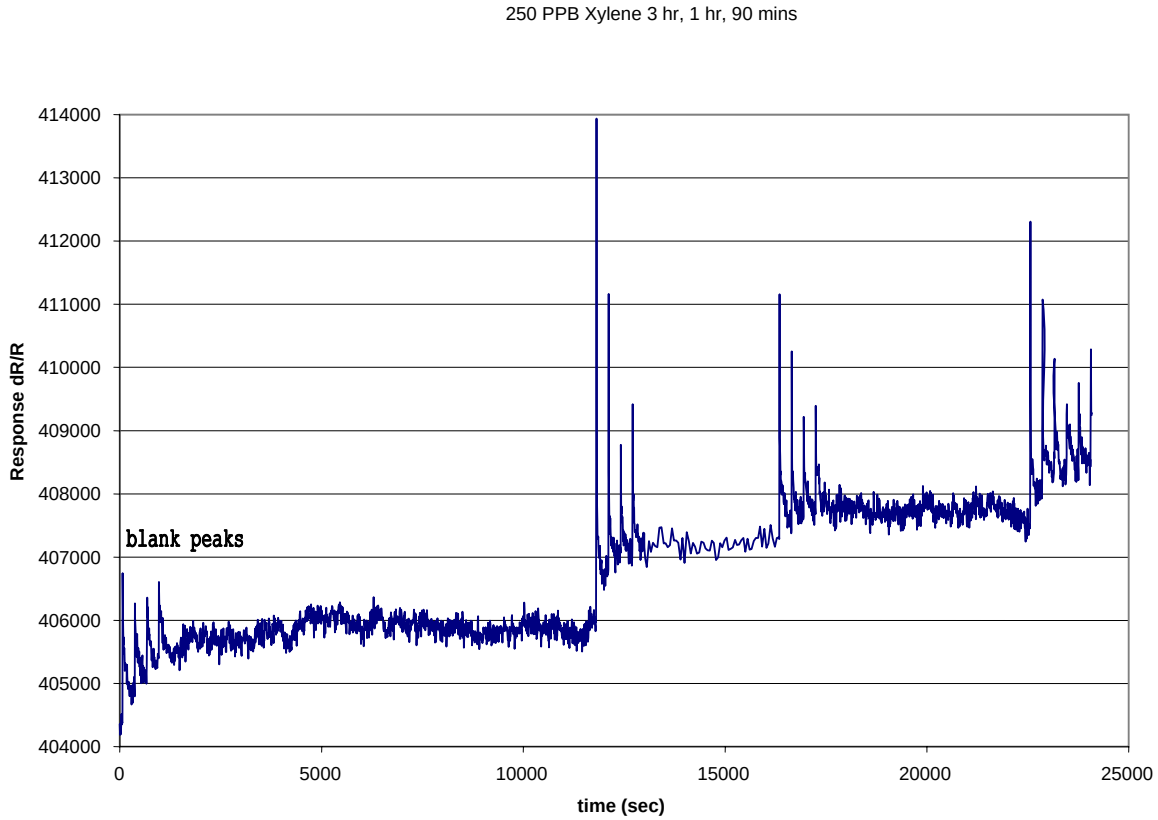

Figure 26. Response of the chemiresistor after loading for 3 hrs, one hour, and 90 minutes respectively at 250 ppb of Xylene in N_2. The initial pulse after loading is followed by 3 clean-out pulses on five-minute intervals before the next loading begins. The chart begins with blank pulses in pure N2 and ends with 2 extra pulses after Xylene was turned off.

3.4 Integrated Chemiresistor-Preconcentrator Probe

In the previous section, the preconcentrator was packaged in a 16-pin DIP separately from the chemiresistor. For site applications, an integrated housing containing both the chemiresistor and preconcentrator is desired. The following section describes the construction, calibration, and testing an integrated chemiresistor-preconcnetrator probe.

3.4.1 Construction of Integrated Preconcentrator/Chemiresistor Probe

A manifold was designed to mate the preconcentrator against the chemiresistor in a face-to-face configuration. The manifold was designed and manufactured utilizing PEEK™ polymer (Polyetheretherketone). The PEEK™ polymer was chosen because of its superior strength, ability to withstand high temperatures (up to 300ºC), and resistance to chemical solvents. The preconcentrator was epoxied in the PEEK™ manifold to create an assembly that can be easily fitted with the chemiresistor (Figure 27). The preconcentrator/PEEK manifold assembly was then mated to the 16-pin DIP with epoxy. The chemiresistor/preconcentrator package was then

placed into the stainless-steel waterproof package and the PC wires were connected to two of the unused wires within the sensor cable (Figure 27).

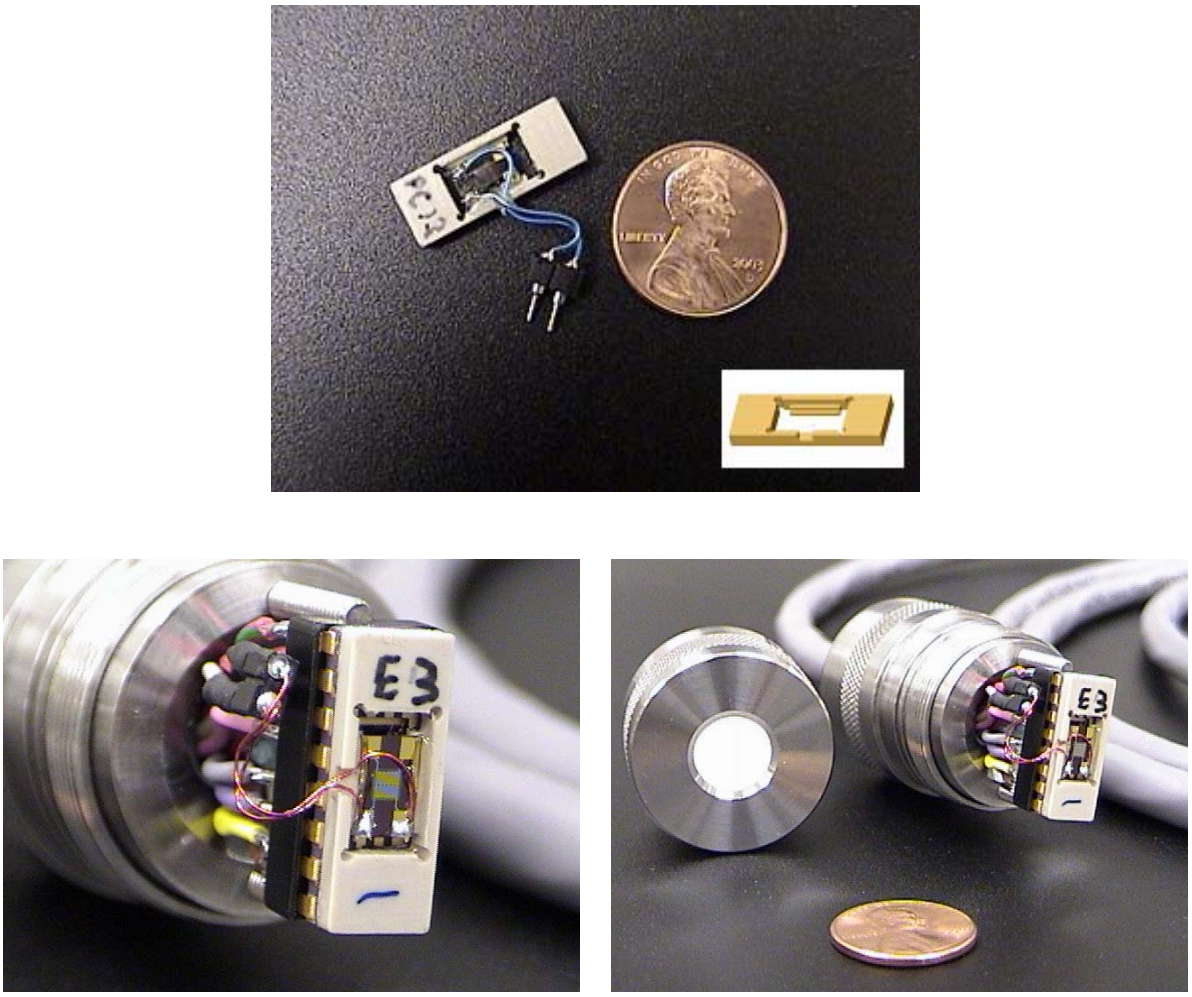

Figure 27. Preconcentrator manifold assembly integrated with the chemiresistor.

3.4.2 Calibration and Testing

This integrated preconcentrator/chemiresistor probe was then calibrated and tested. Figure 28 shows the setup used to test the preconcentrator/chemiresistor assembly. Two gas cylinders, one with dry air and one containing a chemical of interest (e.g., TCE, m-Xylene), were used in conjunction with flow meters on each output to allow for multiple concentrations by controlling the output of each bottle (e.g., TCE (50ppm bottle) and dry air mixed at equal amounts on each flow meter would generate a concentration of 25ppm. The concentration was then monitored by an MTI M200 Micro Gas Chromatograph. The flow was then divided into three different flow streams. To assure equal flow through each apparatus, adjustable flow control valves were placed before each apparatus in conjunction with three flow meters down stream from the

apparatus. Each sensor is placed into an apparatus and monitored by a Campbell Scientific, CR5000 Measurement and control system. The CR5000 also controls the 5 volts applied to the preconcentrator by turning on and off the CR5000 switched 12 volt output. The switched 12 volt output ran through a 3 terminal positive voltage regulator (P/N:NTE960, Specs: V_o:5V, I_o:1A , P_D:15W, V_{in}:35V Max). When the switched 12 volts, from the CR5000, was applied to the input of the regulator, the voltage regulator generated an output of 5 volts, which was applied to the preconcentrator.

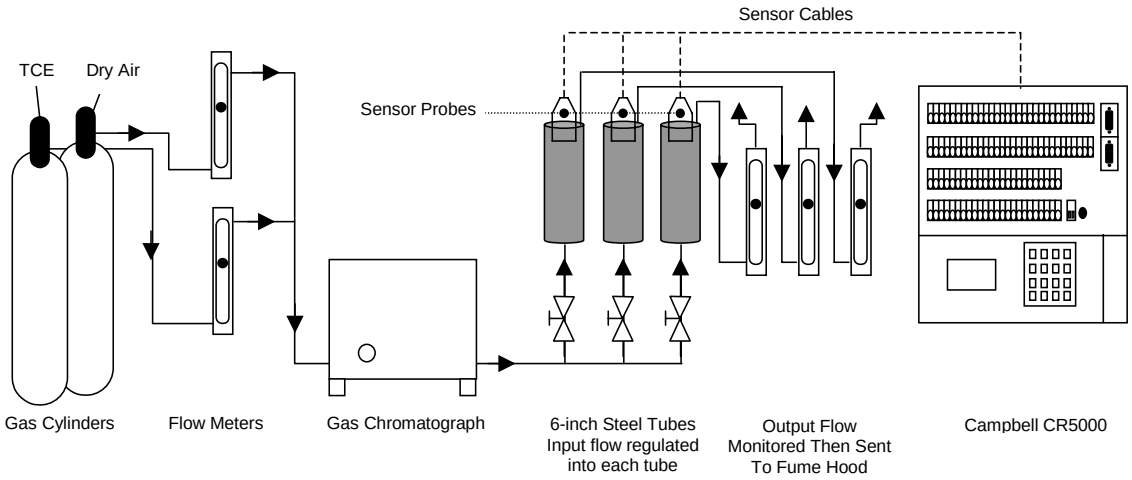

Figure 28. Calibration and testing setup for the preconcentrator/chemiresistor assembly.

A series of purge (pre-fire) pulses were needed to clear the preconcentrator of any previously accumulated chemicals. All pulses were 5 seconds in duration. As shown in Figure 29, the process started with a series of five pre-fire pulses to purge the preconcentrator. Data was collected during the pre-fire period. After the fifth pre-fire pulse a 15-minute load time was started. One minute prior to the "Subtraction or Concentration" pulse, data collection was initiated at a rate of 1 data point every second for 60 seconds. Prior to the last pre-fire (<20msec) pulse the sample rate was stepped up to a rate of 1 data point every 20 millisecond (50/sec) for 10 seconds for 500 data points. The sample rate was stepped back down to a rate of 1 data point every second for 200 seconds for a total of 760 data points over a 4 minute and 30 second period. Varying the data collection rate allowed us to insure that we caught the pulse peek while voltage was applied to the preconcentrator. Additionally, it also enabled us to keep the total number of data points to a minimum for processing purposes.

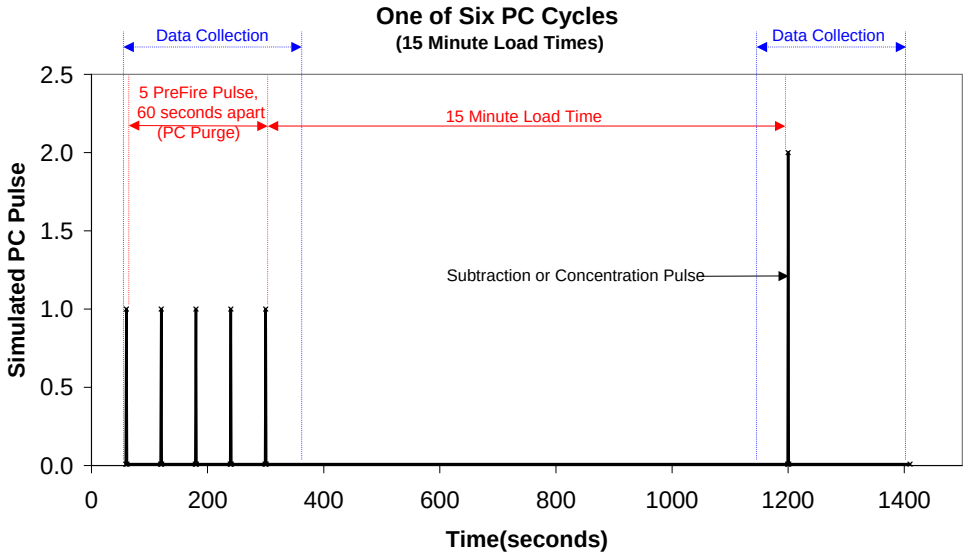

Figure 29. One of six total cycles used during calibration of the preconcentrator (PC)

Figure 30 shows all six cycles of the experiment. The first cycle consisted of five pre-fire pulses followed by a 15-minute load at which time a subtraction pulse was initiated. The subtraction pulse was a resistance measurement, with 5 volts applied, taken over a period of time while exposing the preconcentrator to dry air. This subtraction pulse was then stored into memory for future use. As soon as the subtraction pulse was complete (5 volt supply turned off), the chemical gas flow was started, which exposed the preconcentrator to the chemical of interest. The chemical gas continued to flow through the apparatus for the duration of the experiment. After the subtraction pulse was complete, the chemiresistor was allowed to stabilize for ~5 minutes. Following this stabilization period, five pre-fire pulses were initiated and a 15-minute exposure to the chemical gas began. At the conclusion of the 15-minute load time, an exposure pulse was initiated. The exposure pulse was a resistance measurement, with 5 volts applied, taken over a period of time while exposing the preconcentrator to a chemical of interest. This exposure pulse was then subtracted from the subtraction pulse and the difference was the influence of the chemical of interest on the preconcentrator and chemiresistor.

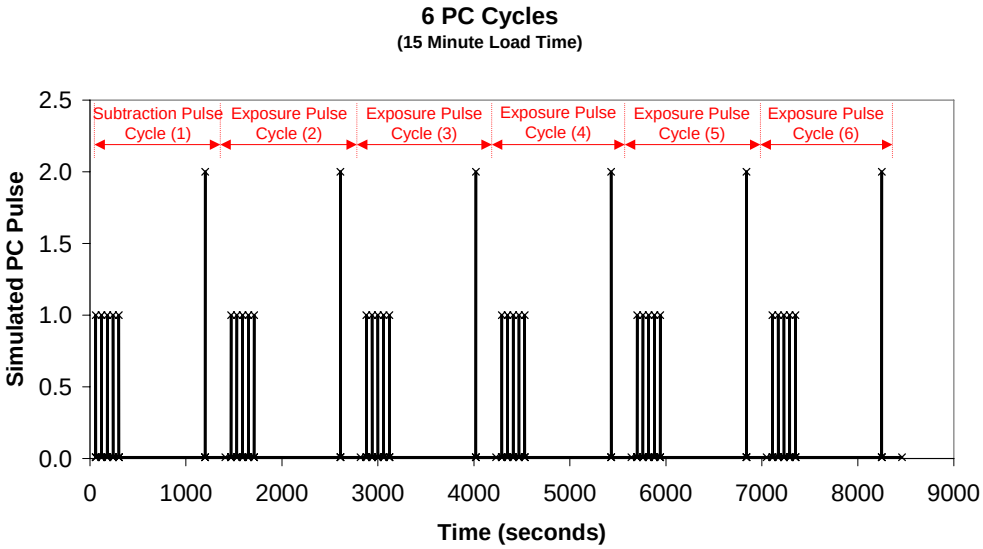

Figure 30. All six cycles with one subtraction pulse and five exposure pulses

3.4.3 Calculation of Confidence Level

The determination of confidence was calculated by taking the standard deviation of a population of 50 data points while dry air was supplied. The 1 value (1 Standard Deviation) was multiplied by two to create a 2 value and by three to create a 3 value. These values were used to calculate the limit of detection at a specific confidence level where 1 : 68%, 2 : 95%, 3 : 99.7%. As seen in figure 31, only four of the fifty data points fell outside the mean ±1 value. In addition, all fifty values fell within the within the Mean ±2 and the Mean ±3 values. Figure 31 (lower left) shows the actual value and its associated tolerance span for each Mean ±(1,2,3) .

One of our concerns was that the individual pulses prior to the TCE pulses might be outside of the established 3σ values. Figure 31 (lower right) shows that only one of our individual subtraction pulses was outside the 3σ values that were established during the 50-noise/detection limit pulses. We also wanted to identify if there was a normal distribution of Max R/Rb values during the 50-noise/detection limit pulses. As seen on the graph, it appears that within 1σ there is a normal distribution of values across the range.

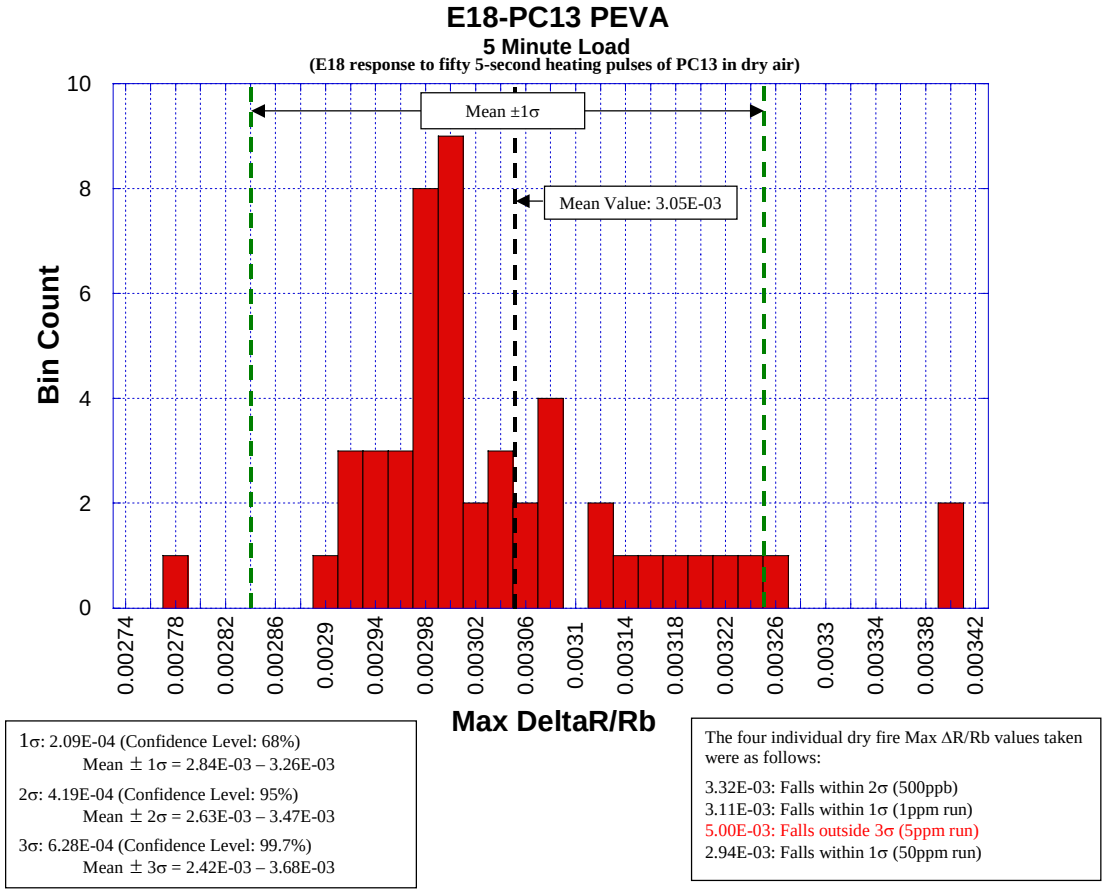

Figure 31. E18-PC13 PEVA histogram of 50 data points with dry air supplied during periodic heating of the preconcentrator

3.4.4 Calibration Results

Calibration of the Chemireisistor/Preconcentrator sensor package consisted of exposing the sensor package to 50ppm, 5ppm, 100ppb, and 50ppb concentrations of TCE over a given amount of time. The data was graphed in TCE concentration as a function of R/Rb. A power trend line ($y=cx^b$, where c and b are constants) was applied to the data points. The 3 value was then applied (x) to the power curve line fit. As seen in Figure 32, the limit of detection for E18-PC13 is 2.2 ppm with a power-law fit.

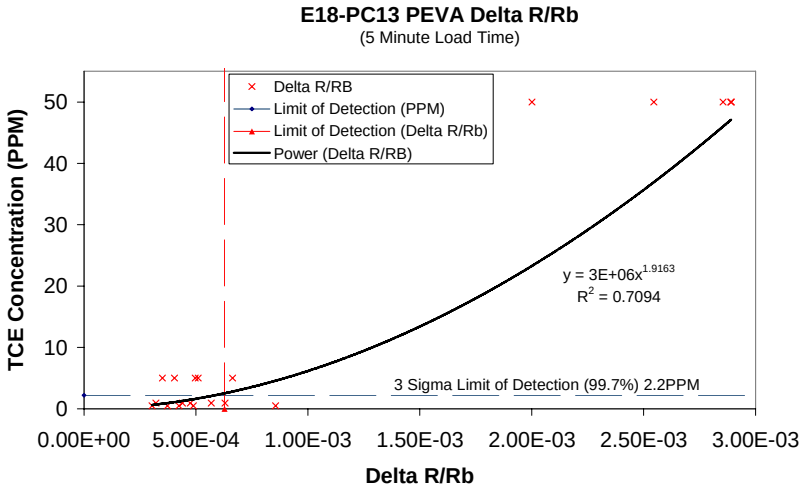

Figure 32. E18-PC13 PEVA calibration to TCE

3.4.5 Hypothesis/Methods of Testing

These tests were conducted with the intention of identifying the different responses between two testing methods. The testing methods were used to identify the re-absorption behavior of the analyte gas onto the preconcentrator following single and multiple pre-fire pulses and to determine whether or not a preconcentrator completely covered with sorbent responds the same as a preconcentrator with only a dot of sorbent. The testing methods included method #1: initial pre-fire pulse only, and method #2: 5 pre-fire pulses to allow the preconcentrator to purge any residual TCE to disperse through the Gore-Tex membrane.

Method #1:
1. Dry air applied
2. Five (5) pre-pulse
3. 15-minute load time
4. 10 baseline readings
5. 5 second pulse at 5-volts (Dry-Heating pulse)
6. TCE (~5ppm) started
7. 15 minute load time
8. 10 baseline readings
9. 5-second pulse at 5-volt (TCE-Heating pulse)
10. Repeat steps 6,7 four more times for a total of 5 TCE-Heating pulses.

Method #2
1. Dry air applied
2. Five (5) pre-pulse
3. 15-minute load time
4. 10 baseline readings
5. 5 second pulse at 5-volts (Dry-Heating pulse)
6. TCE (~5ppm) started
7. Five (5) pre-pulses

8. 15 minute load time
9. 10 baseline readings
10. 5-second pulse at 5-volt (TCE-Heating pulse)
11. Repeat steps 6-8 four more times for a total of 5 TCE-Heating pulses.

Method #1utilized only one pre-fire pulse to purge the preconcentrator sorbent prior to the baseline pulse. As can be seen in Figure 33, there is apparent drift after the concentration pulse. In contrast, method #2 utilized five pre-fire pulses to purge the PC sorbent prior to the dry fire pulse. As seen in Figure 34, a purging pulse appears to create a much more stable and clean pulse.

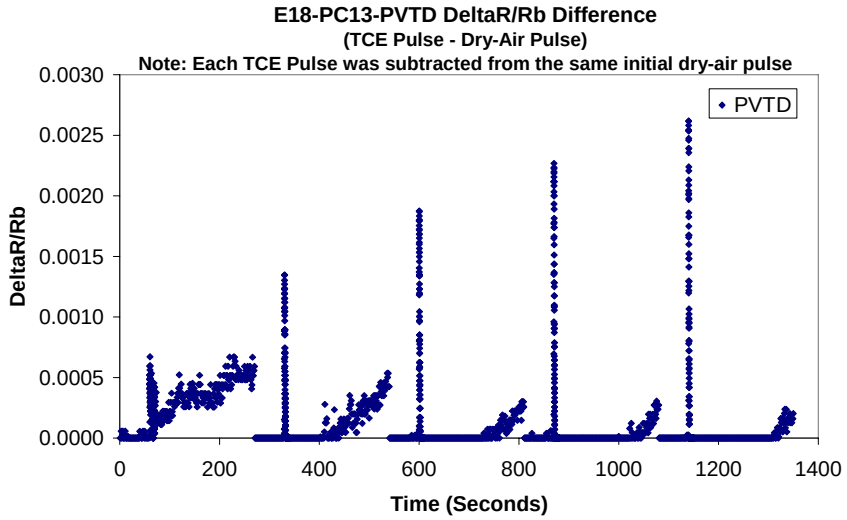

Figure 33. E18-PC13-PVTD response to Method #1.

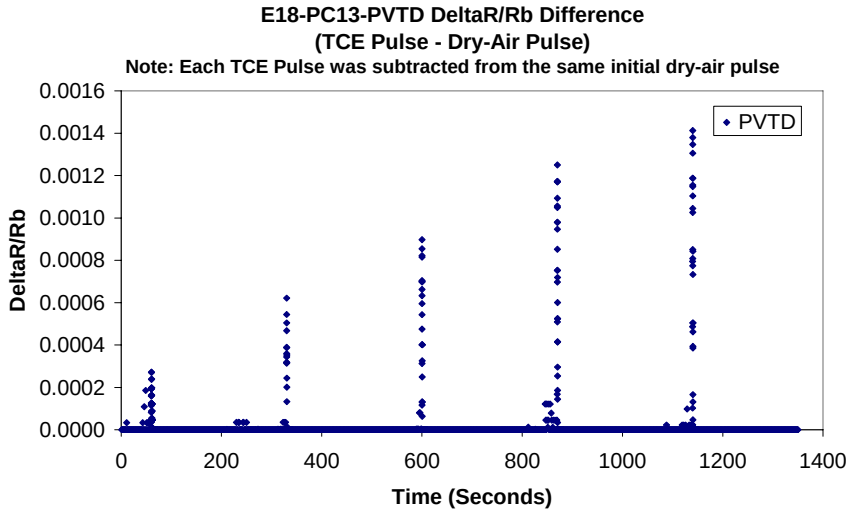

Figure 34. E18-PC13-PVTD response to Method #2

The results of the ΔR/Rb Max values are shown in Figure 35. The response is greater without pre-fire pulses than with pre-fire pulses. This could be due to re-sorption of VOC onto the preconcentrator. It was noticed that the polymer reached equilibrium more rapidly during method 2. With these issues in mind it has been decided that the five pre-fire pulses, prior to the subtraction pulse, would be the best method for future testing. Also, it was noted that the preconcentrator completely covered with Carboxen 1003 provided erratic results compared to that with dot deposition.

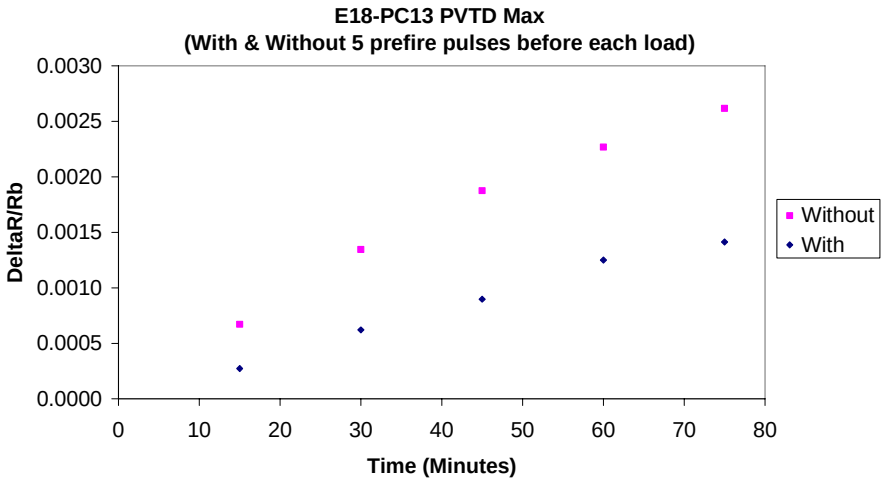

Figure 35. E18-PC13-PVTD maximum changes in relative resistance.

3.4.6 Data Processing

The data was gathered by collecting the resistance readings (*R*) from the chemiresistor and subtracting the average of ten (10) baseline values taken just prior to the pre-fire pulse. This baseline average (*Rb*) is then used to calculate *R/Rb*, where $\Delta R = R - Rb$.

$$\Delta R / R_b Diff = \left(TCEPulse\left[\Delta R / Rb = \frac{R - Rb}{Rb} \right] \right) - \left(DryAirPulse\left[\Delta R / Rb = \frac{R - Rb}{Rb} \right] \right) \qquad (8)$$

This process is done for both the subtraction and the concentration pulses. Only one subtraction pulse is taken under dry air conditions. The subtraction is followed by a 15-minute load time, and then the concentration pulse is initiated. Four more concentration pulses are completed and subtracted from the initial subtraction and a new *R/Rb Diff* values is calculated

3.4.7 Stabilization Testing

The initial stabilization testing was performed after the preconcentrator was allowed to sit for more than 24 hours in ambient conditions. The preconcentrator was pulsed with 5 volts for 5 seconds and 15 minutes apart. This test was conducted to identify the point at which the preconcentrator produced consistent pulse heights. Preconcentrator PC13 mounted on chemiresistor E18 produced expected results. With each recurrent pulse, the response of chemiresistor R/Rb dropped until it reached a stable and consistent reading. In contrast, preconcentrator PC14 mounted on chemiresistor E22 produced erratic results. PC14 showed results that were not expected; with each recurrent pulse the preconcentrator did not drop and reach a stable and consistent reading (Figure 36). From the figure, we have determined that at the sixth pulse, the preconcentrator would reach a fairly stable condition. At this point the preconcentrator would be considered purged and further loading could be performed.

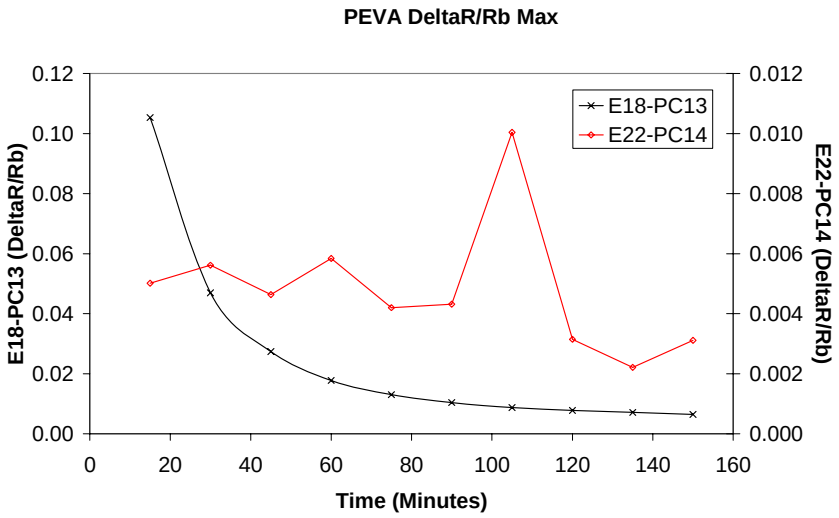

Figure 36. Stabilization test to determine number of purges required to clean the preconcentrator.

3.4.8 Different Load-Time Testing

This test was conducted to identify if different load times would affect the pulse height. The test was started with a pre-fire process to ensure that the preconcentrator was purged of any unknown airborne contaminants. The preconcentrator was then allowed to load for 60 minutes and then pulsed. This process continued successively with 30, 15, 5, 5, 15, 30, 60-minute load time. Figure 37 shows the results of the test.

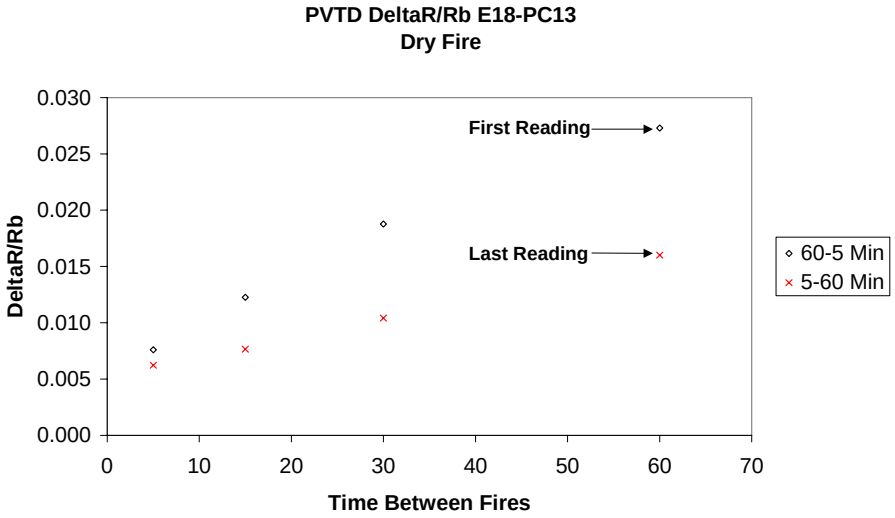

Figure 37. Sensitivity to different load times.

Preconcentrator PC13 mounted on chemiresistor E18 again produced expected results; the responses of chemiresistor ΔR/Rb increased with the load time increase. The difference in the responses for the same load times may be attributed to the previous load time in the sequence. For example, the response of the E18-PC13 60-minute load time shows a difference of ~.01 R/Rb. The load time prior to the first reading was 60 minute and the load time prior to the last reading was 30 minutes.

Preconcentrator PC14 (with the carbon spread over the entire membrane) mounted on chemiresistor E22, however, produced erratic results. The erratic reading of PC E22-PC14 could be attributed to the increased thermal mass of the preconcentrator at its outer edges. The preconcentrator had very little thermal mass on the membrane itself, but at the outer edges of the preconcentrator the thermal mass increases due to the increased amount of silicon. This could cause inconsistent heating of the preconcentrator, which would cause inconsistent purging of the TCE from the Carboxen and erratic readings by the chemiresistor.

3.4.9 Degradation of Preconcentrator

Initial testing of the Preconcentrator indicated decreased response of the Carboxen after a number (>5000) pulses, which indicated the need to further explore the expected life span of a preconcentrator in relation to potential aging processes. The test was preformed by comparing the initial pictures of the preconcentrator to the pictures taken after a long period of use. The Preconcentrator was tested under atmospheric conditions; (~25%RH), 100% helium, and dry air (0%RH). The test was conducted by taking an initial picture of the preconcentrator and then applying a given number of pulses. The pulses were repeated in 2 minute time intervals with each pulse at 5 volts for 5 seconds. The first tests were conducted were under atmospheric conditions. Pictures were taken at 0, 100, and 2500 pulses. The 100% helium and dry air test consisted of pictures being taken at 0 and 2500 pulses.

The test results for the atmospheric conditions are shown in Figure 38. Under atmospheric conditions, the carboxen 1003 film deposited on the preconcentrator gradually fell off between 100 and 2500 pulses. No degradation was observed before 100 pulses. In contrast, little or no degradation of carboxen 1003 films was observed between 0 and 2500 pulses under both dry air and 100% helium conditions. This is probably due to the lack of water under these conditions.

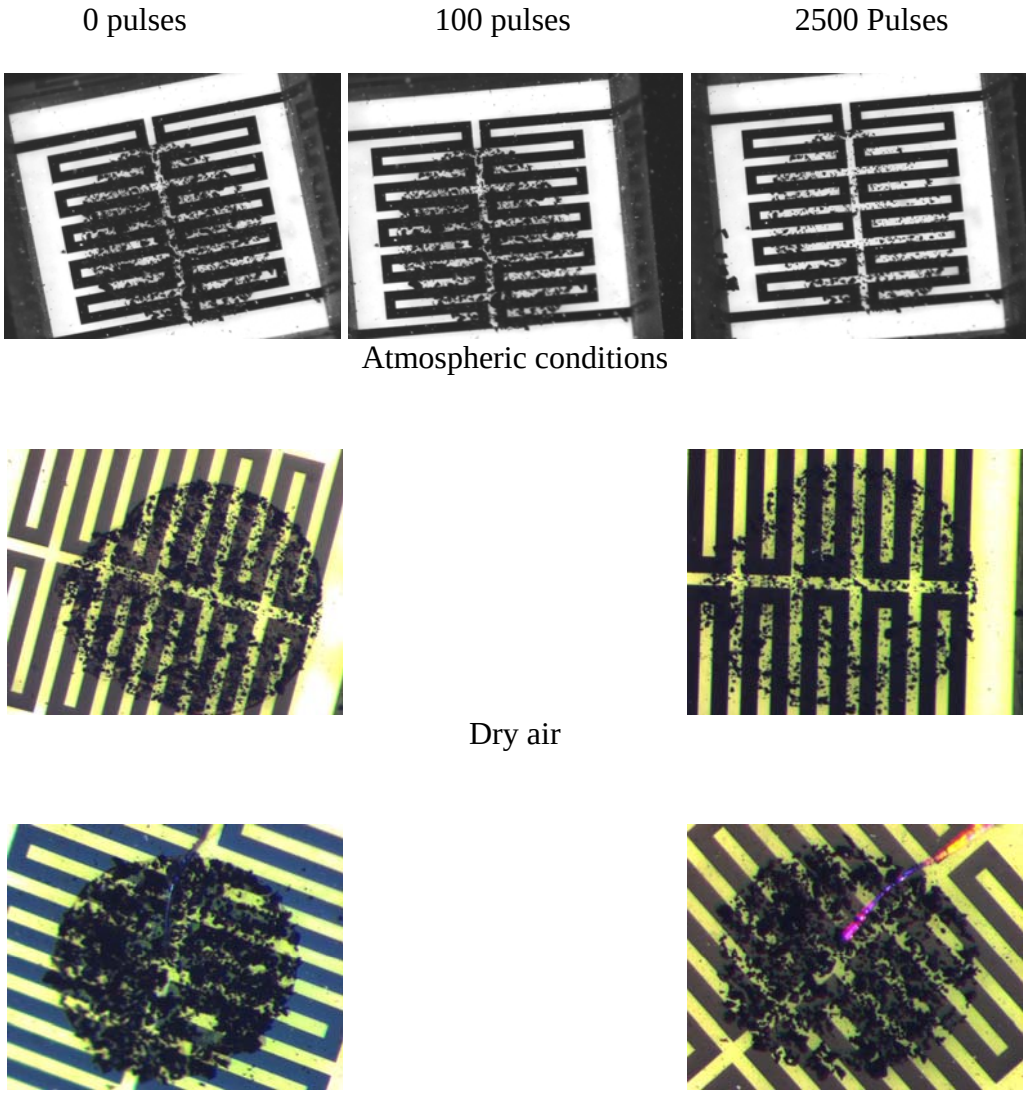

Figure 38. Degradation of preconcentrator due to repeated pulses

4. Hydrogen Sensors

4.1 Mechanism of Hydrogen Sensor

A few years ago a new type of H_2 sensor was invented and developed at Sandia, based on an all solid-state, silicon based microsensor (Hughes, et al., 1989, 1994)]. After much development it was licensed and is being sold as a commercial product by H2SCAN LLC of Valencia, CA. The microelectronic design offers many advantages over previously available H_2 sensors based on other principles, including the common electrochemical cells using liquid electrolytes. These advantages include low cost production, low power requirement and operation in a wide range of ambient temperatures. The new capabilities made it possible to consider the use of this H_2 sensor in a variety of point sensing applications, such as monitoring the evolution of H_2 from mixed waste either in the waste containers themselves or in a storage facility.

The sensor is based on some principles discovered by Lundstrom's group in Sweden in the 1970's (Lundstrom et al. 1989). They found that Pd films as elements in microelectronic devices acted as very sensitive sensors for H_2. The mechanism is a little complicated, but is itself based on the well known catalytic chemistry of Pd and H_2: Molecular H_2 in the gas phase will dissociate on a Pd surface into adsorbed H atoms (Ha), where the fraction of the surface covered by Ha is proportional to the H_2 partial pressure and temperature. H atoms will also occupy sites in the bulk of the Pd metal, with a concentration again proportional to the H_2 partial pressure. At higher H_2 partial pressures a phase transition in the metal occurs creating a new chemical compound, the metal hydride. A huge change in the volume of a film of Pd occurs upon hydride formation due to the large uptake of H_2, and thin films will blister and be destroyed by the hydriding process. This is obviously bad for a thin film sensor, so the Sandia devices take advantage of Pd alloys that don't form the hydrid under normal operating conditions.

There are two sensing mechanisms used in the Sandia sensor: For low concentrations the Pd alloy thin film is used as a field plate for a silicon field effect device (transistor or capacitor). It senses the surface occupation by Ha by a shift in the device characteristics. It can sense concentrations down to about 1 ppm of H_2 in air, and even lower in inert atmospheres. It will sense all concentrations up to 100% H_2, but the response characteristic is logarithmic in H_2 concentration which hurts the accuracy for the critical region around the explosive mixtures of H_2 (4% in air). Improved accuracy in that region is obtained by another sensor on the same chip: a resistor made from the same Pd alloy thin film. By measuring the bulk resistance of the film, accurate values of the higher H_2 concentrations are obtained, since the resistance increases linearly with the square root of the H_2 partial pressure. The result is a device with wide range capabilities, from 1 ppm to 100% H_2, with on-chip temperature control [www.H2SCAN.com].

There are many issues involved with using these devices in different environmental conditions. One that comes up often is operation in an air environment where the H_2 and O_2 can react on the surface of the Pd alloy. This is the common water-forming reaction, but it does cause a change in the calibration curves for both kinds of H_2 sensing devices (Hughes, 1994). This effect has been known for some time and usually it is known in the application whether normal background air is present so the correct calibration curve can be used. If the O_2 partial pressure is

not known, then a separate O_2 sensor is used to assure that the correct calibration curve is used for H_2 concentrations.

4.2 VOC Interference

One of the objectives of this research was to determine if the H2SCAN sensor system would operate reliably in the conditions anticipated for radioactive waste management. To this end, an H2SCAN Hand Held Unit was purchased and tested. The initial test indicated that several VOCs interfered with the calibration curve for the H_2 sensor in air. There was no response to the VOCs by themselves, and virtually no interference when no O_2 was present with the H_2. The effect was not too large, roughly giving a 20% error in the H_2 reading in air (high). The effect was also very non-linear, saturating at a low concentration of VOC (about 1% P/Psat). An example of one of the data runs is given in Figure 39. The red triangles and the right hand scale show the response of the H2SCAN unit. It can be seen that the device is somewhat out of calibration after about 1 year of service: The 1% H_2 in air signal should read exactly "1" when in calibration. The left hand scale shows the % change in resistance of resistor 16.3. Both sensors show and increase in signal when TCA (trichloroethane) is introduced. The hypothesis was that the VOC was interfering with the H_2-O_2 reaction on the Pd alloy surface. No concentration of VOC caused the signal to increase beyond the H_2 signal with no O_2 present.

4.3 Fabrication of Hydrogen Sensor and the Improvement

In an attempt to block the interference of VOCs with the sensor response to H_2-O_2 mixtures, we had two resistive sensors coated with a standard silicon dioxide thin film. This process is well calibrated and used on an almost daily basis in microelectronic chip fabrication in Sandia National Laboratories. The process involves a PECVD (plasma-enhanced-chemical vapor deposition) of a mixture of SiH_4 and N_2O in a He carrier gas. The sensor substrates were heated to 250°C and the bonding pads were protected by a mask. Two sensors were fabricated, one with a 60 nm thick film and the other with a 100 nm film. These films are known to be very dense, not porous. Transmission Electron Microscopic (TEM) pictures obtained at University of New Mexico on witness plates made at the same time as the sensor coatings show the non-porous nature of the films.

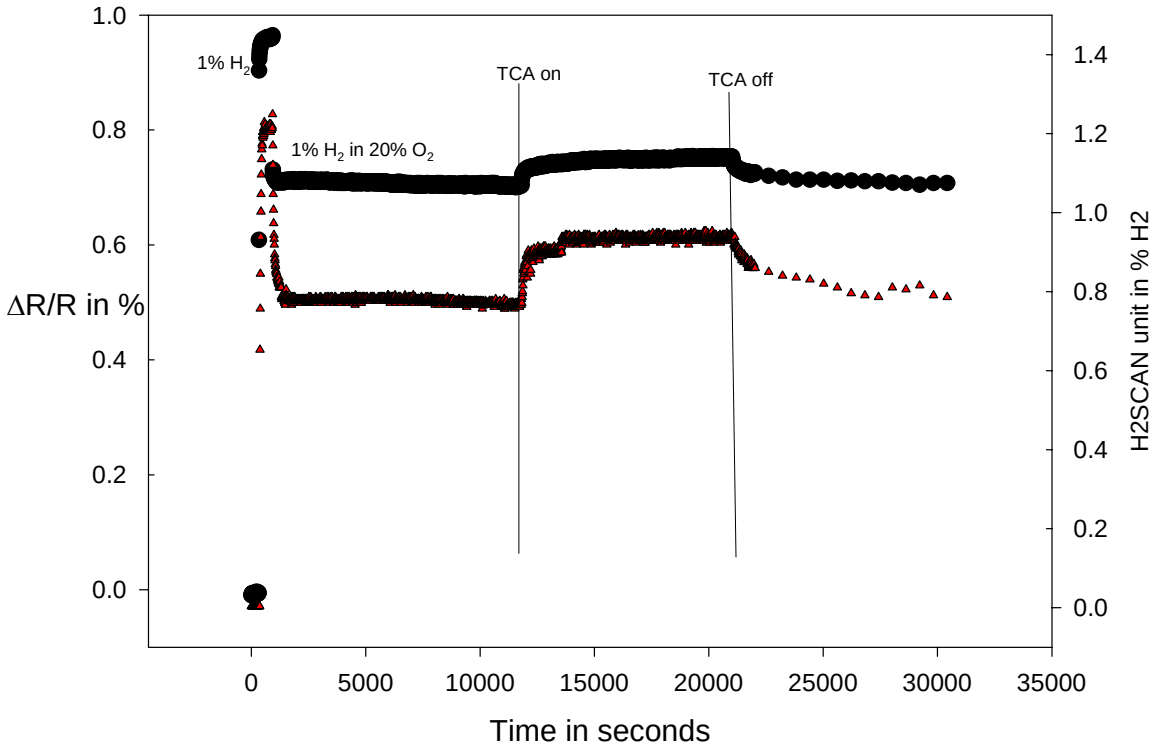

Figure 39. Interference of H_2 sensor readings by TCA. This data run was made on 4-29-03 and shows a comparison of the H2SCAN commercial H2 sensor and a stand-alone resistor with the title "16.3". This resistor had been previously studied in 1997 and 1998 and was coated with a liquid phase sol-gel and then annealed. Results of those tests can be found in ref. [China]. The H2SCAN is exposed to the same analyte flow as the 16.3 which is inside the oven at 80C. The sequence of vapor exposures are: synthetic air to 1 % H2 in N2, to 1%H2 in synthetic air for some 3 hours to reach steady state. The H2SCAN unit had not been calibrated since purchase (2-26-02) so the read-out value of 0.8 % is somewhat low. At about 3 hours a bubbler introduced a 1% (by volume) concentration of the saturated vapor pressure of TCA. It can be seen that the output signal of both sensors are increased by the presence of the TCA. The error introduced by the VOC is about 11% high when the signal increase is put in the calibration curve for 16.3 in air.

4.4 Testing Hydrogen Sensor

4.4.1 Oxygen interference

The resistor sensors, similar to ones shown in Boyle, et al's report (1999) were annealed and tested for speed of response and sensitivity before being coated. The response times for

pulses of 3% H_2 were on the order of a few seconds. After coating the response times are about a factor of 100 slower, possibly due to diffusion of H_2 through the films. However it should be noted that there was little dependence of the response time on the film thickness. This means that it is also possible that the slow step in the response is due to site blockage on the Pd alloy surface, rather than diffusion. The sensitivity to H_2 was about the same. We were disappointed to find that the dense films do not prevent the interference of O_2 on the H_2 signal. The data on sensor 8.1 (60 nm oxide film) is shown in Figure 40. Each data point is 10 sec apart, so the slowness of response to the 3 % H_2 pulse can be seen (black dots). The response of the H2SCAN unit is also shown on the same run as the red triangles with right hand scale. After the 3% H_2 in N_2 pulse, a mixture of 1% H_2 in synthetic air is introduced, and allowed to flow over one hour to make sure that steady state is reached. The O_2 causes a drop in signal on 8.1 from 0.73 to 0.6 at the 1% H_2 concentration. The calibration curves for the coated and uncoated sensor 8.1 are given in Figure 41.

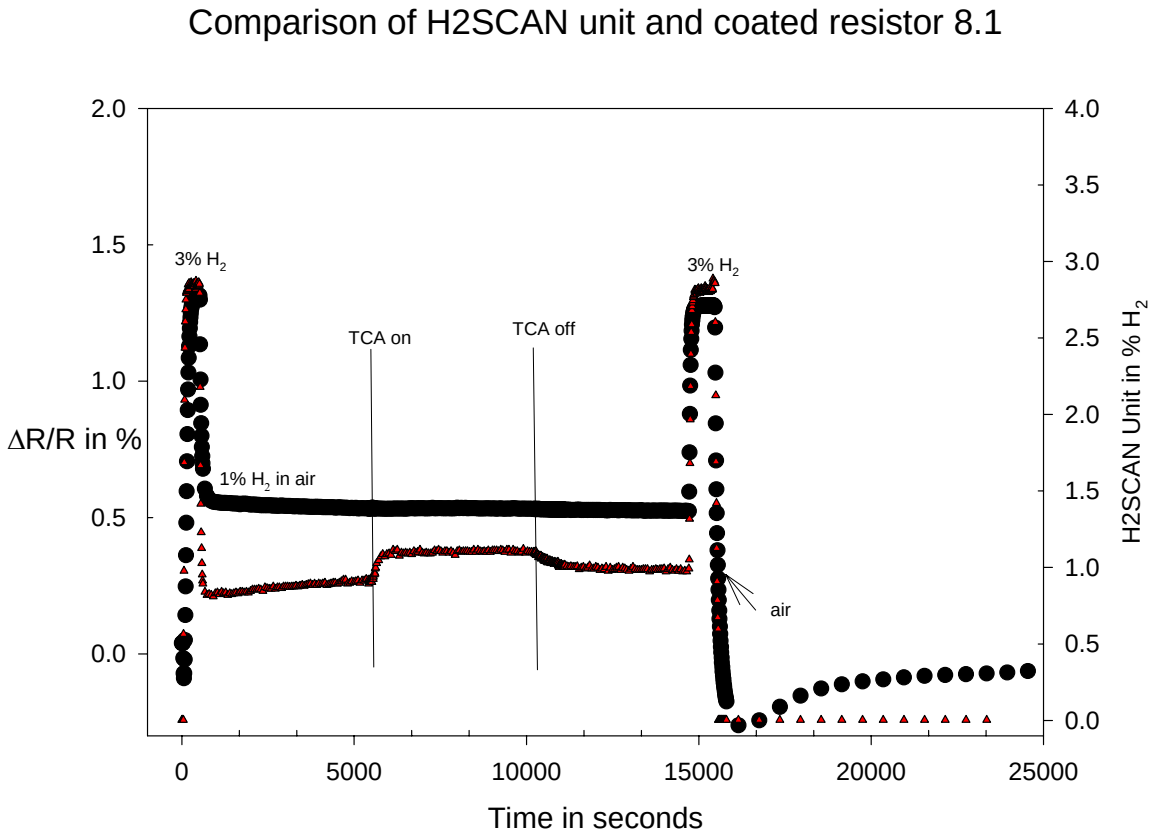

Figure 40. A comparison of the TCA interference on the same H2SCAN unit with a resistor titled "8.1" which has a 60 nm layer of high density PECVD SiO2 deposited on it. This data is taken on 2-27-04, almost a year after the data in Fig. 6. The H2SCAN unit has not been recalibrated and has drifted slightly in the one year period, reading 0.9 % for the 1% H2 in air mixture after about 2 hours of settling. The TCA exposure at the same 1% level produces the same general effect on the reading of the H2SCAN as in the Fig. 6 data (about 20% error high). However the TCA has little effect on the signal from the coated resistor 8.1.

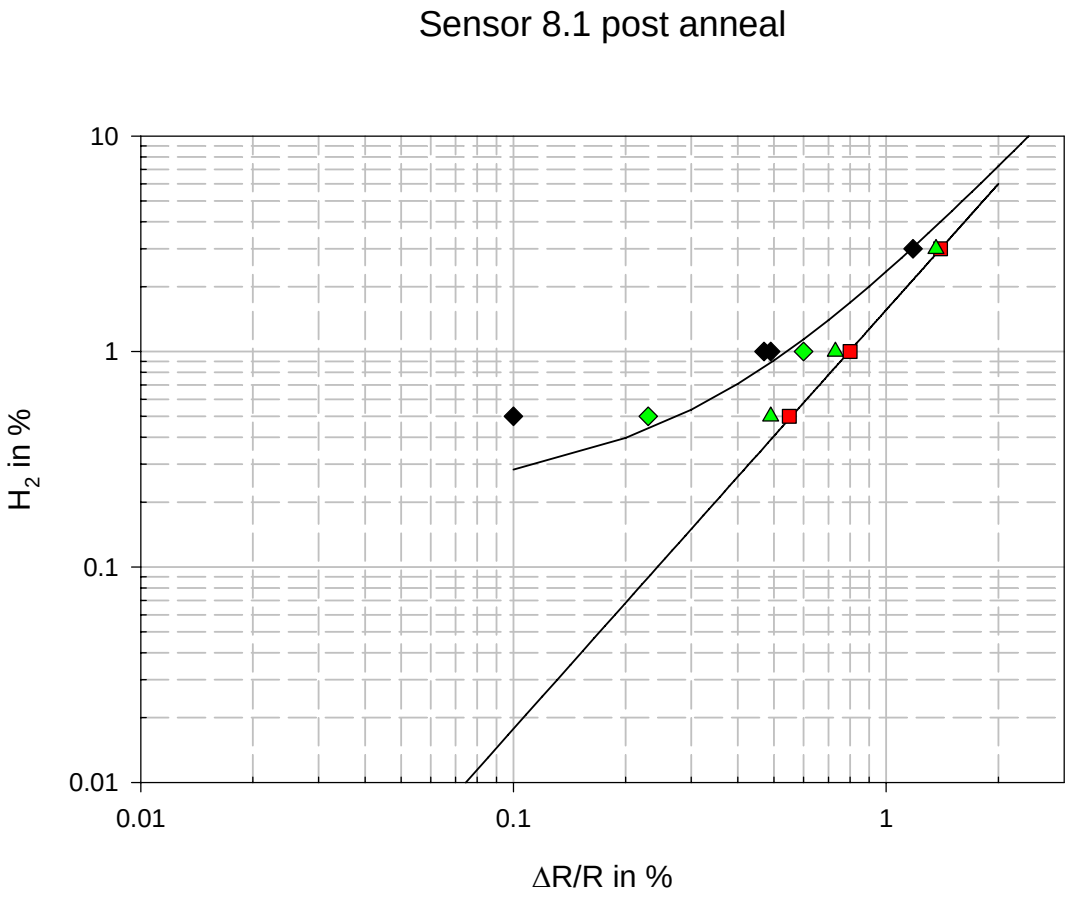

Figure 41. Calibration curves for sensor 8.1 before and after coating with PECVD SiO_2. The red boxes are for the precoating and is fit with the power law: f(x) =1.56*x^1.94, with x being the R/R in % and f(x) being the pH_2 in %. The fit is the solid line through the red boxes. The green triangle shows the small effect of the coating. The prefactor becomes 1.95 and the exponent is 1.8 for best fit (not plotted). The presence of 20% O_2 always lowers the R/R for a given pH_2 concentration. The coating had a large effect in that case as shown by the green diamonds. The fit with the additional term is now: f(x)=1.95*x^1.8 + 0.4*x^0.2, shown by the solid line. For the uncoated device the additional prefactor is 1 and the exponent is 0.4; the data is labeled by black diamond.

4.4.2 Elimination of VOC interference

After the sensors were equilibrated with the 1%H_2 in air mixture, a vapor stream from a bubbler of 1,1,1, trichloroethane (TCA) was mixed in to give a concentration of 1% of the saturated vapor pressure (about 10,000 ppm), keeping the other concentrations constant. In Figure 40, this time is designated as "TCA on". As with the earlier results in Figure 39, the H2SCAN unit shows a positive going response to the TCA, giving an error of about 20% higher H_2 concentration. However, the coated sensor, 8.1 shows no response to the TCA (Figure 40). This is the desired result: no interference of TCA with the H_2 calibration curve in air. Similar

results were obtained with 10% P/Psat of TCA The other coated sensor, 8.4, showed a small response to TCA.

At the line “TCA off” the VOC was removed from the vapor mixture and it can be seen that the H2SCAN unit slowly recovers from the exposure. At about 15000 sec the vapor mixture is changed to 3% H_2 in N2 for comparison to the original 3% H_2 pulse. It can be seen that the TCA exposure had little permanent effect on the sensor responses.

5. Summary

Waste characterization is probably the most costly part of radioactive waste management. An important part of this characterization is the measurements of headspace gas in waste containers in order to demonstrate the compliance with Resource Conservation and Recovery Act (RCRA) or transportation requirements. The traditional chemical analysis methods, which include all steps of gas sampling, sample shipment and laboratory analysis, are expensive and time-consuming as well as increasing worker's exposure to hazardous environments. Therefore, an alternative technique that can provide quick, in-situ, and real-time detections of headspace gas compositions is highly desirable. This report summarizes the results obtained from a Laboratory Directed Research & Development (LDRD) project entitled "Potential Application of Microsensor Technology in Radioactive Waste Management with Emphasis on Headspace Gas Detection". The objective of this project is to bridge the technical gap between the current status of microsensor development and the intended applications of these sensors in nuclear waste management. The major results are summarized below:

- A literature review was conducted on the regulatory requirements for headspace gas sampling/analysis in waste characterization and monitoring. The most relevant gaseous species and the related physiochemical environments were identified. It was found that pre-concentrators might be needed in order for chemiresistor sensors to meet desired detection limits.
- A long-term stability test was conducted for a polymer-based chemresistor sensor array. Significant drifts were observed over the time duration of one month. Such drifts should be taken into account for long-term in-situ monitoring.
- Several techniques were explored to improve the performance of sensor polymers. It has been demonstrated that freeze deposition of black carbon (CB)-polymer can effectively eliminate the so-called "coffee ring" effect and lead to a uniform distribution of CB particles in sensing polymer films. The optimal ratio of CB/polymer has been determined. UV irradiation has also been shown to improve sensor sensitivity.
- From a large set of commercially available polymers, five polymers were selected to form a sensor array that was able to provide optimal responses to six targetVOCs. A series of tests on the sensor array response to various VOC concentrations have been performed. Linear sensor responses have been observed over the tested concentration ranges, although the responses over a whole concentration range are generally nonlinear.
- Inverse models have been developed for identifying individual VOCs based on sensor array responses. A linear solvation energy model is particularly promising for identifying an unknown VOC in a single-component system. It has been demonstrated that a sensor array as such we developed is able to discriminate waste containers for their total VOC concentrations and therefore can be used as screening tool for reducing the existing headspace gas sampling rate.
- Various VOC preconcentrators have been fabricated using Carboxen 1003 as absorbent. Extensive tests have been conducted in order to obtain optimal configurations and parameter ranges for preconcentrator performance. It has been shown that use of preconcentrators can reduce the detection limits of chemiresistors by two orders of magnitude. The life span of preconcentrator under various physiochemical conditions has also been evaluated.

- The performance of Pd film-based H_2 sensors in the presence of VOCs has been evaluated. The interference of the sensor reading by VOC has been observed, which can be attributed to the interference of VOC with the H_2-O_2 reaction on the Pd alloy surface. This interference can be eliminated by coating a layer of silicon dioxide on sensing film surface.

Our work has demonstrated a wide range of applications of gas microsensors in radioactive waste management. Such applications can potentially lead to a significant cost and risk reduction for waste characterization.

6. References

Abraham, M. H., J. Andonian-Halftvan, C. M. Du, V. Diart, G. S. Whiting, J. W. Grate, and R. A. McGill. 1995. Hydrogen bonding. Part 29. Characterization of 14 sorbent coatings for chemical microsensors using a new salvation equation. *Journal of Chemical Society - Perkin Transactions 2*, 369-378.

Abraham, M. H., J. Andonian-Halftvan, G. S. Whiting, A. Leo, and R. S. Taft. 1994. Hydrogen bond. Part 34. The factors that influence the solubility of gases and vapours in water at 298K, and a new method for its determination. *Journal of Chemical Society - Perkin Transactions, 2*, 1777-1790.

Albert, K. J., N. S. Lewis, C. L. Schauer, G. A. Sotzing, S. E. Stitzel, T. P. Vaid, and D. R. Walt. 2000. Cross-reactive chemical sensor arrays. *Chemical Reviews*, 100, 2595-2626.

Boyle, T. J, T. J. Gardner, R. C. Hughes, C. J. Brinker and A. G. Sault. 1999. Catalytic Membrane Sensors. A Thin Film Modified H2 Resistive Sensor for Multi-Molecular Detection. *Comments on Inorganic Chemistry*, 20, 209-231.

Deegan, R. D., O. Bakajin, T. F. Dupont, G. Huber, S. R. Nagel, and T.A Witten. 2000. Contact line deposits in an evaporating drop. *Physical Review*, 62, 756-765.

Eastman, M. P., R. C. Hughes, G. Yelton, A. J., Ricco, S. V. Patel, and M. W. Jenkins. 1999. Application of the solubility parameter concept to the design of chemiresistor arrays. *Journal of the Electrochemical Society*, 146, 3907-39013.

Foulger, S. H. 1999. Reduced percolation thresholds of immiscible conductive blends. *J. Polymer Science*, 37, 1899-1910.

Gonuguntla, M and A. Sharma. 2004. Polymer patterns in evaporating droplets on dissolving substrates. *Langmuir*, 20, 3456-3463.

Grate, J. W., B. M. Wise, and M H. Abraham. 1999. Method for unknown vapor characterization and classification using a multivariate sorption detector. Initial derivation and modeling based on polymer-coated acoustic wave sensor arrays and linear solvation energy relationships. *Analytical Chemistry*, 71, 4544-4553.

Grate, J. W., S. J. Patrash, S. N. Kaganove, M. H. Abraham; B. M. Wise, and N. B.Gallagher. 2001. Inverse least-squares modeling of vapor descriptors using polymer-coated surface acoustic wave sensor array responses. *Analytical Chemistry*, 73, 5247-5259.

Ho, C. K, M. T. Itamura, M. Kelley, and R. C. Hughes. 2001. *Review of Chemical Sensors for In-Situ Monitoring of Volatile Contaminants*. Sandia National Laboratories, Albuquerque, NM. SAND2001-0643.

Ho, C.K., and R.C. Hughes, 2002, *In-Situ* Chemiresistor Sensor Package for Real-Time Detection of Volatile Organic Compounds in Soil and Groundwater, 2002, *Sensors*, 2, 23-34.

Ho, C. K., L. K. McGrath, C.E. Davis, M.L. Thomas, J.L. Wright, A.S. Kooser, and R.C. Hughes. 2003. *Chemiresistor Microsensors for In-Situ Monitoring of Volatile Organic Compounds: Final LDRD Report*, SAND2003-3410, Sandia National Laboratories, Albuquerque, NM.

Hughes, R. C., P. A. Taylor, A. J. Ricco, and R. R. Rye. 1989. Kinetics of hydrogen adsorption and absorption: catalytic gate mis gas sensors on silicon, *J. Electrochem. Soc*. 136, 2653.

Hughes, R. C., D. J. Moreno, M. W. Jenkins, and J. L. Rodriguez. 1994. The Response Of the Sandia robust wide range hydrogen sensor to H_2 -O_2 mixtures. *Technical Digest, Solid State Sensor and Actuator Workshop* (Hilton Head Island, South Carolina, June 13-16), 57-60.

Hughes, R.C., S. A. Casalnuovo, K. O. Wessendorf, D. J. Savignon, D.J., S. Hietala, S. V. Patel, and E. J. Heller. 2000. Integrated chemiresistor array for small sensor platforms. *SPIE Proceedings Paper* 4038-62, p. 519, AeroSense 2000, April 24-28, 2000, Orlando, Florida.

Knite, M, V. Teteris, B. Polyakov, and D. Erts. 2002. Electric and elastic properties of conductive polymeric nanocomposites on macro- and nanoscales. *Materials Science and Engineering C*, 19, 15-19.

Lundstom, I., M. Armgarth, and L.-G. Peterson. 1989. *CRC Crit. Rev. Solid State Mater. Sci*, 15, 201.

Lu, C. J. and E. T. Zellers. 2002. Multi-adsorbent preconcentration/focusing module for portable-GC/microsensor-array analysis of complex vapor mixtures. *Analyst*, 127, 1061-1068.

Manginell, R. P., G. C. Frye-Mason, R. J. Kottenstette, P. R. Lewis, and C. Channy Wong. 2000. Microfabricated planar preconcentrator. *Technical Digest. Solid-State Sensor and Actuator Workshop*, 4-8 June 2000, Hilton Head Island, SC, USA, p.179-82

McGill, R. A., M. H. Abraham, and J. W. Grate. 1994. Choosing polymer coatings for chemical sensor. *Chemtech*, Sept. 27-37.

Medalia, A. I. 1985. Electrical conduction in carbon black composites. *Rubber Chemistry and Technology*, ACS April 23-26, 1985 B.432-454.

Patel, S. V., M. W. Jenkins, R. C. Hughes, W. G. Yelton, and A. J. Ricco. 2000. Differentiation of chemical components in a binary solvent vapor mixture using carbon/polymer composite-based chemisresistor. *Anal. Chem*., 72, 1532-1542.

Ricco, A. J., R. M. Crooks, and G. C. Osbourn. 1998. Surface acoustic wave chemical sensor arrays: New chemically sensitive interfaces combined with novel cluster analysis to detect volatile organic compounds and mixtures. *Acc. Chem. Res*., 31, 289-296.

Federal Agency

Margaret Chu, Director
Office of Civilian Radioactive Waste Management
1000 Independence Avenue
Room 5A-085
Washington, D. C. 20585

Laboratory

James L. Conca
Los Alamos National Labortory
115 Main Street
Carlsbad, NM 88220

Universities

Huifang Xu
Department of Geology and Geophysics
University of Wisconsin
Madison, WI 53706, USA

Enrique Merino
Department of Geology
Indiana University
1005 E. Tenth Street
Bloomington, IN 47405

Libraries

Thomas Branigan Memorial Library
200 Picacho Avenue
Las Cruces, NM 88001

Government Publications Department
Zimmerman Library
University of New Mexico
Albuquerque, NM 87131

New Mexico Tech
Martin Speere Memorial Library
801 Leroy Place
Socorro, NM 87801

Internal Addresses

MS	Org.	
0724	6000	Les Shephard
0771	6800	Dennis L. Berry
0701	6100	Peter Davies
1399	6850	S. Andrew Orrell
1395	6820	Paul E. Shoemaker
0776	6852	M. Kathryn Knowles
1399	6853	Mel Marietta
1395	6821	David S. Kessel
1395	6822	Mark Rogali
0779	6849	Hong-Nian Jow
0778	6851	Peter Swift
1399	6855	Cliff Howard
0778	6851	Robert J. Mackinnon
0771	6853	Frank D. Hansen
1395	6822	Laurence H. Brush
0779	6849	Robert C. Moore
0776	6852	Yifeng Wang (23 copies)
1395	6822	Huizhen Gao
0778	6855	Charles Bryan
0778	6851	Carlos F. Jove-Colon
0778	6855	Russell L. Jarek
0887	1800	Wendy R. Cieslak
0918	10740	Susan Y. Pickering
0750	6118	Tom Hinkebein
0750	6118	James Krumhansl
0750	6118	Patrick Brady
0750	6118	Malcolm Siegel
0750	6118	Randall T. Cygan
0735	6115	Ray Finley
0735	6115	Clifford K. Ho
0735	6115	Jerome L. Wright
0735	6115	Lucas McGrath
1425	1774	Robert C. Hughes
1425	1774	M. Thomas, 1744
0720	6804	Phillip I. Pohl

1	MS 9018	Central Technical Files, 8945-1
2	MS 0899	Technical Library, 9616
3	MS 0323	LDRD Office